Spin-orbit coupling from a two-component self-consistent approach. II. Non-collinear density functional theories

Spin-Orbit Coupling from a Two-Component Self-Consistent Approach. Part II: Non-Collinear Density Functional Theories

Jacques K. Desmarais,[1, 2, a)] Stanislav Komorovsky,[3] Jean-Pierre Flament,[4] and Alessandro Erba[1, b)]
[1)] *Dipartimento di Chimica, Università di Torino, via Giuria 5, 10125 Torino, Italy*
[2)] *Université de Pau et des Pays de l'Adour, E2S UPPA, CNRS, IPREM, Pau, France*
[3)] *Institute of Inorganic Chemistry, Slovak Academy of Sciences, Dúbravská cesta 9, SK-84536 Bratislava, Slovakia*
[4)] *Université de Lille, CNRS, UMR 8523 — PhLAM — Physique des Lasers, Atomes et Molécules, 59000 Lille, France*

(Dated: 30 October 2021)

We revise formal and numerical aspects of collinear and non-collinear density functional theories in the context of a two-component self-consistent treatment of spin-orbit coupling. Theoretical and numerical analyses of the non-collinear approaches confirms their ability to yield the proper collinear limit and provide rotational invariance of the total energy for functionals in the local-density or generalized-gradient approximations (GGA). Calculations on simple molecules corroborate the formal considerations and highlight the importance of an effective screening algorithm to provide the sufficient level of numerical stability required for a rotationally invariant implementation of non-collinear GGA functionals. The illustrative calculations provide a first numerical comparison of both previously proposed non-collinear formulations for GGA functionals. The proposed screening procedure allows to effectively deal with points of small magnetization, which would otherwise be problematic for the evaluation of the exchange-correlation energy and/or potential for non-collinear GGA functionals. Both previously suggested formulations for the non collinear GGA are confirmed to be adequate for total energy calculations, provided that the screening is achieved on a sufficiently fine grid. All methods are implemented in the CRYSTAL program.

Keywords: non-collinear DFT, relativistic DFT, spin-orbit coupling, collinear limit, rotational invariance

I. INTRODUCTION

The Kohn-Sham Density Functional Theory (KS-DFT) is the *de facto* workhorse for studying extended systems from a first principles approach. Calculations on such extended systems are usually performed within the collinear approach to KS-DFT first suggested by Von Barth and Hedin.[1] In this theory, the exchange-correlation (xc) energy E_{xc} depends in a local, semi-local, or non-local way on the electron density n and only one of the three Cartesian components of the electron magnetization $\underline{\mathbf{m}} = [m_x, m_y, m_z]$, typically chosen along the z Cartesian axis (i.e., $E_{xc} = E_{xc}[n, m_z]$).

Despite the success of the collinear approach, the limitation of expressing the xc energy as a functional of only one of the three Cartesian components of the magnetization can be insufficient in certain cases, including geometrically frustrated states of matter. Such states are found, for example, in the naturally occuring face-centered-cubic phase of bulk Fe, and minerals of the Jarosite and Garnet families, which exhibit the ideal Kagomé lattice (in the surface), or the hyper-Kagomé lattice (in the bulk).[2–6] These materials carry states that can be described from a scalar-relativistic (SR) Hamiltonian that includes an electron-electron operator which depends explicitly on spin. But perhaps more importantly, the collinear xc energy expressions are also insufficient for describing fermionic systems if other spin-dependent operators are present in the Hamiltonian, the most notable example being the spin-orbit coupling (SOC) operator.

Indeed if the Hamiltonian depends on spin, the total energy obtained from a collinear xc expression will change according to the direction of the spin-quantisation axis. An arbitrary choice of the z axis for spin quantisation means that the results of a collinear calculation would vary according to the orientation of the Cartesian frame (the calculation is said to not be rotationally invariant). The development of non-collinear (NC) approaches, on the other hand, represent efforts to restore the rotational invariance by instead writing the xc energy as a functional of all three Cartesian components of the magnetization (i.e. $E_{xc} = E_{xc}[n, m_x, m_y, m_z]$).[7–20]

The NC approaches provide a starting point for developing calculation methods based on more rigorous DFTs for treating fermionic systems in a fully-relativistic context (i.e. including both scalar-relativistic and spin-orbit coupling effects). Indeed, if the relativistic Hamiltonian is written in a four-component spinor basis, then the appropriate formulation is the so-called four-current DFT (i.e., $E_{xc} = E_{xc}[\boldsymbol{\mathcal{J}}]$).[21–23] If it is instead written in a two-component spinor basis, then the appropriate relativistic formulation is the spin-current DFT (SCDFT), in which the xc energy depends on not only the elec-

[a)] Electronic mail: jacqueskontak.desmarais@unito.it
[b)] Electronic mail: alessandro.erba@unito.it

tron density and magnetization, but also the three components of the orbital-current density $\mathbf{j} = [j_x, j_y, j_z]$ and a total of nine components from the three spin-current densities $\mathbf{J}_i = [J_{ix}, J_{iy}, J_{iz}]$, $i = x, y, z$ (i.e., $E_{xc} = E_{xc}[n, m_x, m_y, m_z, \mathbf{j}, \mathbf{J}_x, \mathbf{J}_y, \mathbf{J}_z]$).[24–27] The apparent daunting task of generalizing NC functionals to also depend on all of the different components of the SOC-induced orbital- and spin-current densities, is however greatly simplified by inclusion of a fraction of exact non-local Fock exchange, through spin-current hybrid functionals in the local-density or generalized-gradient approximations (LDA or GGA) of the SCDFT, as was recently shown by some of the present authors.[28] The use of such hybrid functionals, however, requires explicitly specifying the non-interacting KS reference as a single Slater determinant. This limitation to a single-reference can be insufficient for systems of strong multi-reference character, especially because of the presence of the spin-dependent SOC operator. In this case, more elaborate multi-reference treatments would be necessary in accordance with the ideas of ensemble DFT.[29–46] The generalization of the SCDFT to a practical calculation approach on such ensembles of interacting electronic states is an open and interesting future research direction.

The most common method to generalize the DFT to NC magnetism is the approach first described by Kübler and co-workers, originally formulated for the LDA and hereafter referred to as the "canonical" NC theory.[7] At variance with the usual collinear theory (where the spin-quantisation axis is taken everywhere along z), the quantisation axis is now allowed to vary from point to point and to locally adopt the direction of the electron magnetization. When used with LDA functionals, the theory is numerically very stable and also reduces properly to the result of the corresponding collinear functional when the magnetization is indeed (anti-)parallel everywhere (the so-called "collinear limit"). Considerable work has also gone towards implementing this formulation for time-dependent DFT.[47–53] Several attempts have been made to generalize this canonical non-collinear theory to functionals beyond the simple LDA.[9,10,12–14,20,54,55] In many cases, serious numerical problems have been reported. Sometimes, these problems have been partly circumvented by throwing away unstable terms in the xc potential.[12–14,20] In other cases, the actual approach used beyond LDA is not entirely outlined,[10] or the numerical instability of the implementation is acknowledged in later publications.[8,9] Moreover, some authors have reported formal problems with the canonical theory, which make generalizations to GGA or meta-GGA functionals to no longer reduce to the collinear limit.[8,11] This apparent lack of reduction to the proper collinear limit was used in part as justification to develop an alternate formulation of the NC approach termed the Scalmani-Frisch (SF) formulation.[8,11] The SF NC theory has been successfully employed in the relativistic calculation of excitation spectra,[17,19,56] and zero field splitting as well as various magnetic properties (EPR, NMR, paramagnetic NMR).[20]

Given the above-mentionned challenges, one consequence is that the rotational invariance of the canonical approach beyond the LDA has not before been studied formally and numerically. Indeed, if the supposed lack of reduction of the canonical NC formulation beyond the LDA to the proper collinear limit were to be true, then the question also arises as to whether this approach is truly rotationally invariant.

Here, we provide thorough formal analysis and illustrative calculations of the NC theories in both the canonical and SF formulations, which show that they achieve the proper collinear limit for LDA and GGA functionals and confirms their rotational invariance. The calculation examples, however, stress the importance of an effective screening algorithm, which is required in practical calculations to achieve the necessary degree of numerical stability for rotational invariance. The illustrative calculations provide a first numerical comparison of previously proposed NC formulations for functionals beyond the LDA. All the formulations of NC-DFT discussed in the paper have been implemented in a developmental version of the public CRYSTAL program.[57]

II. FORMAL ASPECTS

We refer to Part I of the paper for the description of the notation, in particular for the adopted notation for vectors and matrices.[58] The present implementation, as described elsewhere in the literature,[28,58–60] is based on a two-component Kramers-unrestricted approach, where SOC, as well as SR effects are both treated self-consistently from relativistic effective-core potential (RECP) operators. These are mono-electronic, non-local operators which enter into the Hamiltonian and are obtained by fitting a set of solid-spherical Gaussian functions to potentials derived from comparatively very accurate all-electron four-component atomic Dirac-Fock calculations.[61,62]

The presence of the SOC operator implies that the eigenfunctions of the Hamiltonian are complex two-component spinors, which, in our case, are in turn expanded as a linear combination of n_f real-atomic orbitals $\chi_\mu(\underline{\mathbf{r}})$:

$$\mathbf{\Psi}_i(\underline{\mathbf{r}}) = \sum_{\mu=1}^{n_f} \left[\begin{pmatrix} c^{\alpha}_{\mu,i} \\ 0 \end{pmatrix} + \begin{pmatrix} 0 \\ c^{\beta}_{\mu,i} \end{pmatrix} \right] \chi_\mu(\underline{\mathbf{r}}) \,, \qquad (1)$$

where $c^{\sigma}_{\mu,i}$ (with $\sigma = \alpha, \beta$) are complex molecular orbital (MO) coefficients that are determined by solving the corresponding self-consistent field (SCF) equations (either Fock or Kohn-Sham). From the subset of occupied two-component MO spinors in Eq. (1), a complex-Hermitian one-particle density matrix is built as:

$$\left[D^{\sigma\sigma'}\right]_{\mu\nu} \equiv \sum_{i}^{occ} c^{\sigma}_{\mu i} \left[c^{\sigma'}_{\nu i}\right]^{*} \,. \qquad (2)$$

In the present implementation in the CRYSTAL code, the χ_μ atomic orbitals are expressed as a linear combination of real solid-spherical Gaussian-type functions up to angular momentum quantum number $l = 4$ (i.e. g-type functions).[63]

A. Fundamental Variables in Relativistic Density Functional Theory

Any practical formulation of the DFT requires a definition of fundamental density variables from which density functional approximations (DFAs) are built. In the four-component approach, the corresponding formulation is based on the four-current $\boldsymbol{\mathcal{J}}$.[21] In the two-component approach, the approriate formulation is the SCDFT,[24–27] whereby the contribution to the functional from the SOC-induced orbital-current $\mathbf{j}$ and spin-current $\mathbf{J}_x$, $\mathbf{J}_y$, $\mathbf{J}_z$ densities can be treated through an inclusion of a fraction of non-local Fock exchange in the Hamiltonian.[28,59]

The remaining ingredients to be considered explicitly are the particle-number (or total) density:[7–16,21,64]

$$n(\underline{\mathbf{r}}) \equiv \sum_{i}^{occ} \mathbf{\Psi}_i^\dagger(\underline{\mathbf{r}}) \mathbf{\Psi}_i(\underline{\mathbf{r}}) \; , \tag{3}$$

and the magnetization vector $\underline{\mathbf{m}}(\underline{\mathbf{r}})$, whose Cartesian components are defined as:

$$m_c(\underline{\mathbf{r}}) \equiv \sum_{i}^{occ} \mathbf{\Psi}_i^\dagger(\underline{\mathbf{r}}) \hat{\boldsymbol{\sigma}}_c \mathbf{\Psi}_i(\underline{\mathbf{r}}) \; , \tag{4}$$

where $c = x, y, z$ labels a Cartesian component and $\hat{\boldsymbol{\sigma}}_c$ are the usual 2×2 complex Pauli matrices given in Eq. (4) of Part I. By introducing the following compact notation:

$$\begin{aligned} n^{\Re}_{\sigma\sigma'}(\underline{\mathbf{r}}) &= \sum_{\mu\nu} \Re\Big[D^{\sigma\sigma'}\Big]_{\mu\nu} \chi_\mu(\underline{\mathbf{r}}) \chi_\nu(\underline{\mathbf{r}}) \; ; \\ n^{\Im}_{\sigma\sigma'}(\underline{\mathbf{r}}) &= \sum_{\mu\nu} \Im\Big[D^{\sigma\sigma'}\Big]_{\mu\nu} \chi_\mu(\underline{\mathbf{r}}) \chi_\nu(\underline{\mathbf{r}}) \; , \end{aligned} \tag{5}$$

the total density and magnetization can be expressed in terms of the elements of the density matrix as follows:[58]

$$n(\underline{\mathbf{r}}) = n^{\Re}_{\alpha\alpha}(\underline{\mathbf{r}}) + n^{\Re}_{\beta\beta}(\underline{\mathbf{r}}) \; ; \tag{6}$$

$$m_x(\underline{\mathbf{r}}) = n^{\Re}_{\beta\alpha}(\underline{\mathbf{r}}) + n^{\Re}_{\alpha\beta}(\underline{\mathbf{r}}) \; ; \tag{7}$$

$$m_y(\underline{\mathbf{r}}) = n^{\Im}_{\beta\alpha}(\underline{\mathbf{r}}) - n^{\Im}_{\alpha\beta}(\underline{\mathbf{r}}) \; ; \tag{8}$$

$$m_z(\underline{\mathbf{r}}) = n^{\Re}_{\alpha\alpha}(\underline{\mathbf{r}}) - n^{\Re}_{\beta\beta}(\underline{\mathbf{r}}) \; . \tag{9}$$

B. Generalized DFT Treatment

We now discuss the treatment of SOC within the DFT in a two-component framework. Here we show how the approach can be generalized to local-density and generalized-gradient approximations (LDA and GGA) of the exchange-correlation (xc) operator, as well as LDA and GGA hybrid functionals, where a fraction a of non-local Fock exchange is included in its definition. That is to say, we are interested in formulations of DFT associated with energy expressions of the form:

$$E = \mathrm{Tr}\left(\mathbf{hD}\right) + \frac{1}{2}\mathrm{Tr}\left(\mathbf{CD}\right) + \frac{a}{2}\mathrm{Tr}\left(\mathbf{KD}\right) + E_{xc} \; . \tag{10}$$

The exact form of the mono-electronic $\mathbf{h}$ matrix elements, and bi-electronic Coulomb $\mathbf{C}$ and exchange $\mathbf{K}$ matrix elements, as well as strategies for calculating the traces above were discussed in Part I.[58] The formal analyses presented here depend on the formulation of the xc approximation (i.e. whether the functional is of LDA or GGA type), but not on the specific form of the functional itself. E_{xc} is the exchange-correlation energy, which is expressed using integrals over space of the exchange-correlation functional F_{xc}:

$$E^i_{xc} = (1-a) \int F_x[\underline{\mathbf{Q}}^i] d\underline{\mathbf{r}} \; + \; \int F_{\mathrm{corr}}[\underline{\mathbf{Q}}^i] d\underline{\mathbf{r}} \; , \tag{11}$$

where the exchange-correlation functional has been written as a sum of exchange F_x and correlation F_{corr} contributions:

$$F_{xc}[\underline{\mathbf{Q}}^i] \equiv F_x[\underline{\mathbf{Q}}^i] + F_{\mathrm{corr}}[\underline{\mathbf{Q}}^i] \; . \tag{12}$$

For $a = 0$, the formalism reduces to that of plain LDA or GGA formulations. In the above, the exchange-correlation functional depends on a set of variables $\underline{\mathbf{Q}}^i$, where i is an index that labels the different formulations (either $i = col$ for the collinear formulation $i = can$ for the canonical NC formulation or $i = sf$ for the SF NC formulation). In the following, we drop the superscript i on all variables other than $\underline{\mathbf{Q}}^i$ for notational convenience. More explicitly, $\underline{\mathbf{Q}}^i$ is spanned by density variables $n^i_\pm$ and gradient variables $\gamma^i_{\pm\pm}$:

$$\begin{aligned} \underline{\mathbf{Q}}^i(\underline{\mathbf{r}}) &= [Q^i_1(\underline{\mathbf{r}}), Q^i_2(\underline{\mathbf{r}}), Q^i_3(\underline{\mathbf{r}}), Q^i_4(\underline{\mathbf{r}}), Q^i_5(\underline{\mathbf{r}})] \\ &= [n^i_+(\underline{\mathbf{r}}), n^i_-(\underline{\mathbf{r}}), \gamma^i_{++}(\underline{\mathbf{r}}), \gamma^i_{--}(\underline{\mathbf{r}}), \gamma^i_{+-}(\underline{\mathbf{r}})] \; . \end{aligned} \tag{13}$$

The density variables $n^i_\pm$ depend on the value of the total density and magnetization at position $\underline{\mathbf{r}}$ in space, while the gradient variables $\gamma^i_{\pm\pm}$ depend on both the value and gradients (with respect to $\underline{\mathbf{r}}$) of the total density and magnetization at position $\underline{\mathbf{r}}$ in space. So the variables $\gamma^i_{\pm\pm}$ are proper to GGA functionals, whereas the $n^i_\pm$ are present in both LDA and GGA functionals. More details on the exact definitions of these variables are provided in the following. In principle, meta-GGA forms of the exchange-correlation operator could also be treated similarly using however a larger set of variables, but we do not discuss these explicitly here.

The Kohn-Sham Hamiltonian is built using the xc potential $\hat{\mathbf{V}}_{xc}$, which is also written as a sum of exchange and correlation contributions:

$$\hat{\mathbf{V}}_{xc}(\underline{\mathbf{r}}) \equiv \hat{\mathbf{V}}_x(\underline{\mathbf{r}}) + \hat{\mathbf{V}}_{\mathrm{corr}}(\underline{\mathbf{r}}) \; , \tag{14}$$

and, within a two-component generalisation of the theory, is given by:[1,7,9]

$$\hat{\mathbf{V}}_{xc}(\underline{\mathbf{r}}) = \mathcal{E}^{xc}(\underline{\mathbf{r}})\hat{\boldsymbol{\sigma}}_0 + \sum_c \mathcal{B}_c^{xc}(\underline{\mathbf{r}})\hat{\boldsymbol{\sigma}}_c \ , \tag{15}$$

where the $\hat{\boldsymbol{\sigma}}_c$ are the 2×2 complex Pauli matrices, $\hat{\boldsymbol{\sigma}}_0$ is the 2×2 identity matrix, and both $\mathcal{E}^{xc}$ and $\mathcal{B}_c^{xc}$ are defined in terms of functional derivatives of the xc energy. More specifically, the xc electrostatic potential $\mathcal{E}^{xc}$ reads:

$$\mathcal{E}^{xc}(\underline{\mathbf{r}}) = \frac{\delta E_{xc}}{\delta n(\underline{\mathbf{r}})} \ , \tag{16}$$

and the Cartesian components $\mathcal{B}_c^{xc}$ of the so-called xc magnetic field read:

$$\mathcal{B}_c^{xc}(\underline{\mathbf{r}}) = \frac{\delta E_{xc}}{\delta m_c(\underline{\mathbf{r}})} \ , \tag{17}$$

where in the expressions above, δ is used to represent the functional derivative.

We can use the $\underline{\boldsymbol{\mathcal{B}}}^{xc}$ to define the local torque of the xc magnetic field $\underline{\boldsymbol{\tau}_{\boldsymbol{xc}}}$ as follows:[65–67]

$$\underline{\boldsymbol{\tau}_{\boldsymbol{xc}}}(\underline{\mathbf{r}}) = \underline{\mathbf{m}}(\underline{\mathbf{r}}) \times \underline{\boldsymbol{\mathcal{B}}}^{xc}(\underline{\mathbf{r}}) \ . \tag{18}$$

The variables $\underline{\mathbf{Q}}^i$ on which the functional depends can in general be chosen such that the $\underline{\boldsymbol{\tau}_{\boldsymbol{xc}}}$ is locally non-vanishing, even though in general its integral over all space $\int \underline{\boldsymbol{\tau}_{\boldsymbol{xc}}}(\underline{\mathbf{r}}) d\underline{\mathbf{r}}$ should be null, such that it obeys the so-called zero-torque theorem.[65–67]

The Kohn-Sham Hamiltonian matrix elements are expressed using mono-electronic (including SR and SOC) and bi-electronic (Coulomb and exchange) integrals, as well as the xc potential $\hat{\mathbf{V}}_{xc}$ introduced above. For the diagonal spin-blocks we have:

$$\begin{aligned}\left[H_{KS}^{\sigma\sigma}\right]_{\mu\nu} = &\left[h^{\sigma\sigma}\right]_{\mu\nu} + \left[C^{\sigma\sigma}\right]_{\mu\nu} + a\left[K^{\sigma\sigma}\right]_{\mu\nu} \\ &+ (1-a)\left[V_x^{\sigma\sigma}\right]_{\mu\nu} + \left[V_{\text{corr}}^{\sigma\sigma}\right]_{\mu\nu} \ .\end{aligned} \tag{19}$$

For off-diagonal spin-blocks (i.e. for $\sigma \neq \sigma'$), all mono-electronic integrals apart from SOC ones are null, as well as the bi-electronic Coulomb integrals (as shown in Part I), so that we have:

$$\begin{aligned}\left[H_{KS}^{\sigma\sigma'}\right]_{\mu\nu} = &\left[h_{\text{SO}}^{\sigma\sigma'}\right]_{\mu\nu} + a\left[K^{\sigma\sigma'}\right]_{\mu\nu} \\ &+ (1-a)\left[V_x^{\sigma\sigma'}\right]_{\mu\nu} + \left[V_{\text{corr}}^{\sigma\sigma'}\right]_{\mu\nu} \ .\end{aligned} \tag{20}$$

The xc potential is described in the following according to two competing theories: the collinear and non-collinear formalisms.[1,7–10,12–14] More details are provided below in Sections II C and II D on the two theories.

C. Collinear Density Functional Theory

In the collinear formalism, the variables $\underline{\mathbf{Q}}^{col}$ entering the exchange-correlation functional depend only on the total density n and z component of the magnetization m_z, while the x and y components of the magnetization are set to zero. As a consequence, the x and y components of the xc magnetic field introduced in Eq. (17) must vanish. From Eq. (15), the xc potential thus reduces to:

$$\hat{\mathbf{V}}_{xc}(\underline{\mathbf{r}}) = \mathcal{E}^{xc}(\underline{\mathbf{r}})\hat{\boldsymbol{\sigma}}_0 + \mathcal{B}_z^{xc}(\underline{\mathbf{r}})\hat{\boldsymbol{\sigma}}_z \ . \tag{21}$$

Given the real nature of both $\hat{\boldsymbol{\sigma}}_0$ and $\hat{\boldsymbol{\sigma}}_z$, the xc potential therefore forms a real block diagonal matrix in spin-space:

$$\mathbf{V}_{xc} = \begin{pmatrix} \mathbf{V}_{xc}^{\alpha\alpha} & \mathbf{0}^{\alpha\beta} \\ \mathbf{0}^{\beta\alpha} & \mathbf{V}_{xc}^{\beta\beta} \end{pmatrix} \ , \tag{22}$$

whose matrix elements are real Hermitian:

$$\left[V_{xc}^{\sigma\sigma}\right]_{\mu\nu} = \left[V_{xc}^{\sigma\sigma}\right]_{\nu\mu} \ . \tag{23}$$

From Eq. (21) and by recalling the definition of the xc electrostatic potential and xc magnetic field given in Eqs. (16) and (17), we get the following expressions for the collinear xc potential in terms of functional derivatives of the xc energy E_{xc}:

$$\hat{V}_{xc}^{\alpha\alpha}(\underline{\mathbf{r}}) = \frac{\delta E_{xc}}{\delta n_{\alpha\alpha}^{\Re}(\underline{\mathbf{r}})} \tag{24}$$

$$\hat{V}_{xc}^{\beta\beta}(\underline{\mathbf{r}}) = \frac{\delta E_{xc}}{\delta n_{\beta\beta}^{\Re}(\underline{\mathbf{r}})} \ . \tag{25}$$

The disadvantage of the collinear theory is that rotational invariance is lost when calculations are performed in the presence of a SOC operator. The loss of rotational invariance means that a rigid rotation of the molecule will cause a change in energy. This occurs because the collinear theory effectively consists of choosing the spin-quantisation axis along z for the xc potential term. Given that the SOC operator imparts an energy dependence on the orientation of the spin-quantisation axis,[58] the arbitrary and non-general choice of the z direction results in loss of rotational invariance.

1. Collinear LDA

As introduced in Section II B, LDA xc functionals only depend on $n_+^i(\underline{\mathbf{r}})$ and $n_-^i(\underline{\mathbf{r}})$, which, in the collinear formalism (in analogy to the non- or scalar-relativistic one-component approach), are defined as:

$$n_+^{col}(\underline{\mathbf{r}}) = n_{\alpha\alpha}^{\Re}(\underline{\mathbf{r}}) \tag{26}$$

$$n_-^{col}(\underline{\mathbf{r}}) = n_{\beta\beta}^{\Re}(\underline{\mathbf{r}}) \ , \tag{27}$$

and are therefore built solely from the real part of the $\alpha\alpha$ and $\beta\beta$ blocks of the density matrix. From Eqs. (6) and (9), the variables above can be shown to depend only on the total density n and z component of the magnetization m_z as:

$$n_\pm^{col}(\underline{\mathbf{r}}) = \frac{1}{2}\left[n(\underline{\mathbf{r}}) \pm m_z(\underline{\mathbf{r}})\right] \ . \tag{28}$$

From calculus of variations, for LDA, the functional derivatives of the energy in Eqs. (24) and (25) reduce to the following partial derivatives of the xc functional:

$$\hat{V}_{xc}^{\sigma\sigma}(\underline{\mathbf{r}}) = \frac{\partial F_{xc}}{\partial n_{\sigma\sigma}^{\Re}(\underline{\mathbf{r}})} \,. \tag{29}$$

2. Collinear GGA

As discussed above, apart from the $n_{\pm}^{i}$ introduced above, GGA xc functionals also depend on gradient variables $\gamma_{\pm\pm}^{i}$, which, within the collinear formalism (again, in analogy to the non-relativistic one-component approach), are defined as:

$$\gamma_{\pm\pm}^{col}(\underline{\mathbf{r}}) = \underline{\hat{\boldsymbol{\nabla}}} n_{\pm}^{col}(\underline{\mathbf{r}}) \cdot \underline{\hat{\boldsymbol{\nabla}}} n_{\pm}^{col}(\underline{\mathbf{r}}) \,. \tag{30}$$

From Eq. (28), it is easy to see that also these variables only depend on the total density n and z component of the magnetization m_z:

$$\gamma_{\pm\pm}^{col}(\underline{\mathbf{r}}) = \frac{1}{4} \underline{\hat{\boldsymbol{\nabla}}} \left[n(\underline{\mathbf{r}}) \pm m_z(\underline{\mathbf{r}}) \right] \cdot \underline{\hat{\boldsymbol{\nabla}}} \left[n(\underline{\mathbf{r}}) \pm m_z(\underline{\mathbf{r}}) \right] \tag{31}$$

For GGA, standard calculus of variations gives the following expression for the xc potential:[68]

$$\hat{V}_{xc}^{\sigma\sigma}(\underline{\mathbf{r}}) = \frac{\partial F_{xc}}{\partial n_{\sigma\sigma}^{\Re}(\underline{\mathbf{r}})} - \underline{\hat{\boldsymbol{\nabla}}} \cdot \left[2 \frac{\partial F_{xc}}{\partial \left| \underline{\hat{\boldsymbol{\nabla}}} n_{\sigma\sigma}^{\Re}(\underline{\mathbf{r}}) \right|^2} \underline{\hat{\boldsymbol{\nabla}}} n_{\sigma\sigma}^{\Re}(\underline{\mathbf{r}}) + \frac{\partial F_{xc}}{\partial \gamma_{+-}^{col}(\underline{\mathbf{r}})} \underline{\hat{\boldsymbol{\nabla}}} n_{\sigma'\sigma'}^{\Re}(\underline{\mathbf{r}}) \right] , \tag{32}$$

where in the equation above $\sigma \neq \sigma'$. From Eq. (32), for GGA functionals the evaluation of the xc potential would require the second derivatives of the xc functional (e.g. one from the $\underline{\hat{\boldsymbol{\nabla}}}$ operator and one w.r.t. γ_{+-}^{col}). However, as was first noted by Pople and co-workers,[68] the matrix elements of the xc potential can be obtained through integration by parts, such that only the first derivatives of the functional are required, as follows:

$$[V_{xc}^{\sigma\sigma}]_{\mu\nu} = \int \frac{\partial F_{xc}}{\partial n_{\sigma\sigma}^{\Re}(\underline{\mathbf{r}})} \chi_\mu(\underline{\mathbf{r}}) \chi_\nu(\underline{\mathbf{r}}) d\underline{\mathbf{r}} \; + \; \int \left[2 \frac{\partial F_{xc}}{\partial \left| \underline{\hat{\boldsymbol{\nabla}}} n_{\sigma\sigma}^{\Re}(\underline{\mathbf{r}}) \right|^2} \underline{\hat{\boldsymbol{\nabla}}} n_{\sigma\sigma}^{\Re}(\underline{\mathbf{r}}) + \frac{\partial F_{xc}}{\partial \gamma_{+-}^{col}(\underline{\mathbf{r}})} \underline{\hat{\boldsymbol{\nabla}}} n_{\sigma'\sigma'}^{\Re}(\underline{\mathbf{r}}) \right] \cdot \underline{\hat{\boldsymbol{\nabla}}} \chi_\mu(\underline{\mathbf{r}}) \chi_\nu(\underline{\mathbf{r}}) d\underline{\mathbf{r}} \,. \tag{33}$$

D. Non-Collinear Density Functional Theory

In the non-collinear formalism, the variables entering the exchange-correlation functional depend on the total density n and on the three Cartesian components of the magnetization $\underline{\mathbf{m}}$, so that rotational invariance is ensured even in the presence of the SOC operator.

Given that the xc functional now depends on the total density and on the three Cartesian components of the magnetization, the non-collinear xc potential has the form shown on Eq. (15) and therefore forms a complex matrix in spin-space:

$$\mathbf{V}_{xc} = \begin{pmatrix} \mathbf{V}_{xc}^{\alpha\alpha} & \mathbf{V}_{xc}^{\alpha\beta} \\ \mathbf{V}_{xc}^{\beta\alpha} & \mathbf{V}_{xc}^{\beta\beta} \end{pmatrix} \,. \tag{34}$$

Based on Eq. (15) and on the expressions for the Pauli matrices, the following symmetry properties can be derived. For the diagonal $\alpha\alpha$ spin-block:

$$\begin{aligned} [V_{xc}^{\alpha\alpha}]_{\mu\nu} &= [V_{xc}^{\alpha\alpha}]_{\nu\mu} \\ &= \langle \chi_\mu | \mathcal{E}^{xc} + \mathcal{B}_z^{xc} | \chi_\nu \rangle \,. \end{aligned} \tag{35}$$

For the diagonal $\beta\beta$ spin-block:

$$\begin{aligned} \left[V_{xc}^{\beta\beta} \right]_{\mu\nu} &= \left[V_{xc}^{\beta\beta} \right]_{\nu\mu} \\ &= \langle \chi_\mu | \mathcal{E}^{xc} - \mathcal{B}_z^{xc} | \chi_\nu \rangle \,. \end{aligned} \tag{36}$$

For the off-diagonal spin-blocks, the matrix elements read as follows:

$$\begin{aligned} \left[V_{xc}^{\alpha\beta} \right]_{\mu\nu} = \left[V_{xc}^{\alpha\beta} \right]_{\nu\mu} = \left[V_{xc}^{\beta\alpha} \right]_{\nu\mu}^{*} = \left[V_{xc}^{\beta\alpha} \right]_{\mu\nu}^{*} \\ = \langle \chi_\mu | \mathcal{B}_x^{xc} - i \mathcal{B}_y^{xc} | \chi_\nu \rangle \,. \end{aligned} \tag{37}$$

So the diagonal $\alpha\alpha$ and $\beta\beta$ spin-blocks of the xc potential are real Hermitian so that only their upper (or lower) triangular parts need to be computed. The off-diagonal $\alpha\beta$ and $\beta\alpha$ spin-blocks are complex symmetric so that only the upper (or lower) triangular part of $\alpha\beta$ needs to be calculated.

Depending on the choice of the variables used in the definition of the xc functional, two different (canonical and SF) formulations of non-collinear two-component DFT are possible. They are both reviewed below.

1. The Canonical Formulation

In the canonical formulation of the non-collinear DFT, the variables on which F_{xc} depends are built starting from the generalized density:[7]

$$\bar{\mathbf{n}}(\underline{\mathbf{r}}) = \frac{1}{2} \left[n(\underline{\mathbf{r}}) \hat{\boldsymbol{\sigma}}_0 + \sum_c m_c(\underline{\mathbf{r}}) \hat{\boldsymbol{\sigma}}_c \right] \,. \tag{38}$$

By recalling the exact form of the Pauli matrices given in Eq. (4) of Part I, the generalized density can be written explicitly as follows in terms of the total density and components of the magnetization:

$$\bar{\mathbf{n}}(\underline{\mathbf{r}}) = \frac{1}{2}\begin{pmatrix} n(\underline{\mathbf{r}}) + m_z(\underline{\mathbf{r}}) & m_x(\underline{\mathbf{r}}) - im_y(\underline{\mathbf{r}}) \\ m_x(\underline{\mathbf{r}}) + im_y(\underline{\mathbf{r}}) & n(\underline{\mathbf{r}}) - m_z(\underline{\mathbf{r}}) \end{pmatrix} . \quad (39)$$

By performing a unitary transformation on the generalized density $\bar{\mathbf{n}}$, which diagonalizes locally in space the matrix above, one gets the $n_{\pm}^{can}$ variables used in the definition of the xc functional:[8,12]

$$\bar{\mathbf{n}}(\underline{\mathbf{r}}) \overset{diag}{=} \begin{pmatrix} n_+^{can}(\underline{\mathbf{r}}) & 0 \\ 0 & n_-^{can}(\underline{\mathbf{r}}) \end{pmatrix} , \quad (40)$$

where the eigenvalues of the matrix are:

$$n_{\pm}^{can}(\underline{\mathbf{r}}) = \frac{1}{2}\left[n(\underline{\mathbf{r}}) \pm m(\underline{\mathbf{r}})\right] , \quad (41)$$

where $m = |\underline{\mathbf{m}}|$ is the magnitude of $\underline{\mathbf{m}}$. Comparison of Eq. (41) with Eqs. (26) and (27), shows that the non-collinear definition of the $n_{\pm}^{can}$ variables differs from the collinear definition by replacing m_z by m (i.e. the z component of the magnetization by the absolute value of the magnetization).

From Eqs. (16) and (17), the xc potential can be written in terms of the $n_{\pm}^{can}$ by noticing that, from the chain rule of differentiation:

$$\frac{\delta E_{xc}}{\delta m_c} = \frac{\delta E_{xc}}{\delta m}\frac{\delta m}{\delta m_c} = \frac{\delta E_{xc}}{\delta m}\frac{m_c}{m} . \quad (42)$$

where from now on the dependence on $\underline{\mathbf{r}}$ is dropped. Finally, using Eq. (38) and taking into account that $n = \mathrm{Tr}\left[\bar{\mathbf{n}}\hat{\boldsymbol{\sigma}}_0\right]$ and $m_c = \mathrm{Tr}\left[\bar{\mathbf{n}}\hat{\boldsymbol{\sigma}}_c\right]$ shows that the xc potential operator can be written more succinctly as a functional derivative of the xc energy with respect to the generalized density:

$$\hat{\mathbf{V}}_{xc} = \frac{\delta E_{xc}}{\delta \bar{\mathbf{n}}} . \quad (43)$$

When considering an LDA xc functional, the functional derivatives of the xc energy in Eqs. (16), (17) and (42) reduce to partial derivatives of the xc functional:

$$\mathcal{E}^{xc} = \frac{\partial F_{xc}}{\partial n} \quad ; \quad \mathcal{B}_c^{xc} = \frac{m_c}{m}\frac{\partial F_{xc}}{\partial m} . \quad (44)$$

In a scalar- or non-relativistic code, the partial derivatives of the xc functional with respect to n and m_z are available. So, for an LDA functional, one has to simply replace m_z by m in the existing code to generalize it to the canonical non-collinear theory.

GGA xc functionals also depend on the gradient variables $\gamma_{\pm\pm}^{i}$ that, within the canonical formulation of non-collinear DFT read:

$$\gamma_{\pm\pm}^{can} = \frac{1}{4}\left\{\hat{\underline{\boldsymbol{\nabla}}}\left[n \pm m\right] \cdot \hat{\underline{\boldsymbol{\nabla}}}\left[n \pm m\right]\right\} , \quad (45)$$

where the gradient of the absolute magnetization is calculated as follows:

$$\hat{\underline{\boldsymbol{\nabla}}} m = \frac{1}{m}\sum_c m_c \hat{\underline{\boldsymbol{\nabla}}} m_c . \quad (46)$$

Later we are going to discuss some numerical issues and corresponding solutions related to the treatment of these terms. For application to GGA functionals, standard calculus of variations leads to the following expressions for the functional derivatives of the xc energy:

$$\mathcal{E}^{xc} = \frac{1}{2}\left\{ \underbrace{\left(\frac{\partial F_{xc}}{\partial n_+^{can}} + \frac{\partial F_{xc}}{\partial n_-^{can}}\right)}_{\Gamma_+} - \hat{\underline{\boldsymbol{\nabla}}} \cdot \underbrace{\left[2\frac{\partial F_{xc}}{\partial \gamma_{++}^{can}}\hat{\underline{\boldsymbol{\nabla}}} n_+^{can} + 2\frac{\partial F_{xc}}{\partial \gamma_{--}^{can}}\hat{\underline{\boldsymbol{\nabla}}} n_-^{can} + \frac{\partial F_{xc}}{\partial \gamma_{+-}^{can}}\left(\hat{\underline{\boldsymbol{\nabla}}} n_+^{can} + \hat{\underline{\boldsymbol{\nabla}}} n_-^{can}\right)\right]}_{\Lambda_+} \right\} ; \quad (47)$$

and:

$$\mathcal{B}_c^{xc} = \frac{m_c}{2m}\left\{ \underbrace{\left(\frac{\partial F_{xc}}{\partial n_+^{can}} - \frac{\partial F_{xc}}{\partial n_-^{can}}\right)}_{\Gamma_-} - \hat{\underline{\boldsymbol{\nabla}}} \cdot \underbrace{\left[2\frac{\partial F_{xc}}{\partial \gamma_{++}^{can}}\hat{\underline{\boldsymbol{\nabla}}} n_+^{can} - 2\frac{\partial F_{xc}}{\partial \gamma_{--}^{can}}\hat{\underline{\boldsymbol{\nabla}}} n_-^{can} - \frac{\partial F_{xc}}{\partial \gamma_{+-}^{can}}\left(\hat{\underline{\boldsymbol{\nabla}}} n_+^{can} - \hat{\underline{\boldsymbol{\nabla}}} n_-^{can}\right)\right]}_{\Lambda_-} \right\} . \quad (48)$$

From Eqs. (35), (36) and (37), we see that the matrix elements of the GGA xc potential are built from $\left[\mathcal{E}^{xc}\right]_{\mu\nu}$ and $\left[\mathcal{B}_c^{xc}\right]_{\mu\nu}$. Through integration by parts, we find the following working expressions:

$$\left[\mathcal{E}^{xc}\right]_{\mu\nu} = \frac{1}{2}\left[\int \chi_\mu\chi_\nu\Gamma_+ d\underline{\mathbf{r}} + \int \Lambda_+ \cdot \hat{\underline{\boldsymbol{\nabla}}}\left(\chi_\mu\chi_\nu\right) d\underline{\mathbf{r}}\right] , \quad (49)$$

and:

$$[\mathcal{B}_c^{xc}]_{\mu\nu} \approx \int \frac{m_c}{2m}\chi_\mu\chi_\nu\Gamma_- d\underline{\mathbf{r}} + \int \frac{m_c}{2m}\Lambda_- \cdot \underline{\hat{\boldsymbol{\nabla}}}\left(\chi_\mu\chi_\nu\right) d\underline{\mathbf{r}}\,, \tag{50}$$

where in the passage from Eq. (48) to Eq. (50), the term originating from the gradient of m_c/m has been dropped. Thus, Eq. (50) represents the commonly adopted approximation, in which the gradient of the magnetization is assumed to locally follow the quantization axis of the magnetization vector for the definition of the xc magnetic field.[12,14,20,55] As will be seen through the numerical examples from Section IV, this approximation does not appreciably affect the rotational invariance or reduction to the collinear limit of the theory. We leave the evaluation of terms arising from the gradient of m_c/m for future work.

2. The Scalmani-Frisch Formulation

Scalmani and Frisch have proposed an alternative formulation of the non-collinear theory, which differs from the canonical theory illustrated above for functionals beyond the LDA.[11] This theory adopts the following definitions for the GGA variables:

$$\gamma^{sf}_{++} \text{ or } \gamma^{sf}_{--} = \frac{1}{4}\left[\underline{\hat{\boldsymbol{\nabla}}}n\cdot\underline{\hat{\boldsymbol{\nabla}}}n + \underline{\hat{\boldsymbol{\nabla}}}\,\underline{\mathbf{m}}\cdot\circ\underline{\hat{\boldsymbol{\nabla}}}\,\underline{\mathbf{m}}\right] \pm \frac{f_\nabla}{2}\underbrace{\left[\left(\underline{\hat{\boldsymbol{\nabla}}}n\cdot\underline{\hat{\boldsymbol{\nabla}}}\,\underline{\mathbf{m}}\right)\circ\left(\underline{\hat{\boldsymbol{\nabla}}}n\cdot\underline{\hat{\boldsymbol{\nabla}}}\,\underline{\mathbf{m}}\right)\right]^{\frac{1}{2}}}_{\Xi} \tag{51}$$

and:

$$\gamma^{sf}_{+-} = \frac{1}{4}\left[\underline{\hat{\boldsymbol{\nabla}}}n\cdot\underline{\hat{\boldsymbol{\nabla}}}n - \underline{\hat{\boldsymbol{\nabla}}}\,\underline{\mathbf{m}}\cdot\circ\underline{\hat{\boldsymbol{\nabla}}}\,\underline{\mathbf{m}}\right]\,, \tag{52}$$

where the dot product identified by the symbol "$\cdot$" runs over the components of $\underline{\hat{\boldsymbol{\nabla}}}$ while that identified by the symbol "$\circ$" runs over the components of $\underline{\mathbf{m}}$. Finally, the f_∇ is defined as:

$$f_\nabla = \mathrm{sgn}\left[\underline{\hat{\boldsymbol{\nabla}}}n\cdot\left(\underline{\hat{\boldsymbol{\nabla}}}\,\underline{\mathbf{m}}\right)\circ\underline{\mathbf{m}}\right]\,, \tag{53}$$

where the signum function "sgn" returns either 1 or -1 according to the sign of the argument. We obtain expressions for the matrix elements of the theory of Scalmani and Frisch from the calculus of variations. We do not show details of the derivation, but report the final expressions, as follows:

$$[\mathcal{E}^{xc}]_{\mu\nu} = \frac{1}{2}\int\Gamma_+\chi_\mu\chi_\nu d\underline{\mathbf{r}} + \frac{1}{2}\int\left\{\left(\frac{\partial F_{xc}}{\partial\gamma^{sf}_{++}} + \frac{\partial F_{xc}}{\partial\gamma^{sf}_{--}} + \frac{\partial F_{xc}}{\partial\gamma^{sf}_{+-}}\right)\underline{\hat{\boldsymbol{\nabla}}}n + \left(\frac{\partial F_{xc}}{\partial\gamma^{sf}_{++}} - \frac{\partial F_{xc}}{\partial\gamma^{sf}_{--}}\right) f_\nabla\,\Xi^{-1}\left(\underline{\hat{\boldsymbol{\nabla}}}n\cdot\underline{\hat{\boldsymbol{\nabla}}}\,\underline{\mathbf{m}}\right)\circ\underline{\hat{\boldsymbol{\nabla}}}\,\underline{\mathbf{m}}\right\}\cdot\underline{\hat{\boldsymbol{\nabla}}}\left(\chi_\mu\chi_\nu\right) d\underline{\mathbf{r}}\,, \tag{54}$$

and:

$$[\mathcal{B}_c^{xc}]_{\mu\nu} \approx \frac{1}{2}\int\frac{m_c}{m}\Gamma_-\chi_\mu\chi_\nu d\underline{\mathbf{r}} + \frac{1}{2}\int\left\{\left(\frac{\partial F_{xc}}{\partial\gamma^{sf}_{++}} + \frac{\partial F_{xc}}{\partial\gamma^{sf}_{--}} - \frac{\partial F_{xc}}{\partial\gamma^{sf}_{+-}}\right)\underline{\hat{\boldsymbol{\nabla}}}m_c + \left(\frac{\partial F_{xc}}{\partial\gamma^{sf}_{++}} - \frac{\partial F_{xc}}{\partial\gamma^{sf}_{--}}\right) f_\nabla\,\Xi^{-1}\left(\underline{\hat{\boldsymbol{\nabla}}}n\cdot\underline{\hat{\boldsymbol{\nabla}}}m_c\right)\underline{\hat{\boldsymbol{\nabla}}}n\right\}\cdot\underline{\hat{\boldsymbol{\nabla}}}\left(\chi_\mu\chi_\nu\right) d\underline{\mathbf{r}}\,. \tag{55}$$

As, was the case for the canonical formulation, also here for the SF formulation Eq. (55) is an approximate expression for the xc magnetic field matrix elements, this time because terms arising from the gradient of f_∇ are not considered — see for instance Eq. (57) of Ref. 19. The numerical examples presented below in Section IV suggest also here that such terms do not have an appreciable effect on the rotational invariance and reduction to the collinear limit of the implementation.

3. Rotational Invariance and Reduction to the Collinear Limit of Non-Collinear Theories

Both the canonical and SF formulations of NC KS-DFT described above in sections II D 1 and II D 2 are at-

tempts to restore rotational invariance to existing DFAs for calculations on systems which can be described by a Hamiltonian that depends explicitly on spin (for instance, containing a SOC operator). Although it is intuitive that the insertion of all three Cartesian components of the magnetization (rather than only one component) into the xc energy expression, could eventually lead to restoring its rotational invariance, a formal proof (or numerical evidence) to support this assumption for functionals beyond the LDA is still lacking. Furthermore, a desirable property of any NC formulation is that it reduces to the corresponding collinear formulation when the magnetization is everywhere (anti)-parallel in space (the so-called "collinear limit"). As a matter of fact, the supposed lack of the proper collinear limit of the canonical NC formulation for functionals beyond the LDA was used in part as justification for providing the SF one.[8,11] If the lack of reduction to the correct collinear limit of the canonical NC formulation were to be true, then the question arises as to whether this approach can in fact be shown to truly be rotationally invariant. In this section, we provide formal arguments to support that both the SF and canonical formulations do indeed reduce to the proper collinear limit for LDA and GGA functionals and, as a consequence, can also be formally characterized as being rotationally invariant.

For providing the formal demonstration, it proves useful to perform a linear transformation which recasts the xc energy expression in Eqs. (11)-(13) not as functional of the variables $\underline{\mathbf{Q}}^i$, but instead using a new set of variables $\underline{\mathbf{P}}^i = [P_1^i, P_2^i, P_3^i, P_4^i, P_5^i]$, in which $i = col$, can, or sf. The relevant transformation is chosen such that:

$$Q_1^i = n_+^i = \frac{1}{2}P_1^i + \frac{1}{2}P_2^i \tag{56a}$$

$$Q_2^i = n_-^i = \frac{1}{2}P_1^i - \frac{1}{2}P_2^i \tag{56b}$$

$$Q_3^i = \gamma_{++}^i = \frac{1}{4}P_3^i + \frac{1}{4}P_4^i + \frac{1}{2}P_5^i \tag{56c}$$

$$Q_4^i = \gamma_{--}^i = \frac{1}{4}P_3^i + \frac{1}{4}P_4^i - \frac{1}{2}P_5^i \tag{56d}$$

$$Q_5^i = \gamma_{+-}^i = \frac{1}{4}P_3^i - \frac{1}{4}P_4^i \tag{56e}$$

Substituting Eqs. (30) and (31) in Eq. (56), we obtain the following for the collinear formulation:

$$\underline{\mathbf{P}}^{col} = [n, m_z, \underline{\hat{\boldsymbol{\nabla}}} n \cdot \underline{\hat{\boldsymbol{\nabla}}} n, \underline{\hat{\boldsymbol{\nabla}}} m_z \cdot \underline{\hat{\boldsymbol{\nabla}}} m_z, \underline{\hat{\boldsymbol{\nabla}}} n \cdot \underline{\hat{\boldsymbol{\nabla}}} m_z] \tag{57}$$

Then, substituting Eqs. (41) and (45) in Eq. (56), we find, for the canonical NC formulation:

$$\underline{\mathbf{P}}^{can} = [n, m, \underline{\hat{\boldsymbol{\nabla}}} n \cdot \underline{\hat{\boldsymbol{\nabla}}} n, \underline{\hat{\boldsymbol{\nabla}}} m \cdot \underline{\hat{\boldsymbol{\nabla}}} m, \underline{\hat{\boldsymbol{\nabla}}} n \cdot \underline{\hat{\boldsymbol{\nabla}}} m] \tag{58}$$

and finally, substituting Eqs. (57)-(59) in Eq. (56), for the SF formulation:

$$\underline{\mathbf{P}}^{sf} = [n, m, \underline{\hat{\boldsymbol{\nabla}}} n \cdot \underline{\hat{\boldsymbol{\nabla}}} n, \underline{\hat{\boldsymbol{\nabla}}}\ \underline{\mathbf{m}} \cdot \circ \underline{\hat{\boldsymbol{\nabla}}}\ \underline{\mathbf{m}}, f_\nabla \Xi] \tag{59}$$

We start by looking at the reduction to the collinear limit and rotational invariance of $E_{xc}[\underline{\mathbf{P}}^{can}]$, then $E_{xc}[\underline{\mathbf{P}}^{sf}]$, respectively for the canonical and SF NC formulations. This is followed by a discussion of the collinear limit and rotational invariance of the corresponding xc potential expressions.

Showing that $E_{xc}[\underline{\mathbf{P}}^{can}]$ reduces to the proper collinear limit for the specific case of strictly positive m_z follows immediately by comparing Eq. (57) with Eq. (58) and noticing that:

$$\begin{aligned}
&\lim_{\underline{\mathbf{m}} \to m_z} E_{xc}[\underline{\mathbf{P}}^{can}] = E_{xc}[\underline{\mathbf{P}}^{can}]\big|_{cl} \\
&= E_{xc}[n, m, \underline{\hat{\boldsymbol{\nabla}}} n \cdot \underline{\hat{\boldsymbol{\nabla}}} n, \underline{\hat{\boldsymbol{\nabla}}} m \cdot \underline{\hat{\boldsymbol{\nabla}}} m, \underline{\hat{\boldsymbol{\nabla}}} n \cdot \underline{\hat{\boldsymbol{\nabla}}} m]\Big|_{cl} \\
&= E_{xc}[n, |m_z|, \underline{\hat{\boldsymbol{\nabla}}} n \cdot \underline{\hat{\boldsymbol{\nabla}}} n, \underline{\hat{\boldsymbol{\nabla}}} |m_z| \cdot \underline{\hat{\boldsymbol{\nabla}}} |m_z|, \underline{\hat{\boldsymbol{\nabla}}} n \cdot \underline{\hat{\boldsymbol{\nabla}}} |m_z|] \\
&\underbrace{=}_{m_z \geq 0} E_{xc}[n, m_z, \underline{\hat{\boldsymbol{\nabla}}} n \cdot \underline{\hat{\boldsymbol{\nabla}}} n, \underline{\hat{\boldsymbol{\nabla}}} m_z \cdot \underline{\hat{\boldsymbol{\nabla}}} m_z, \underline{\hat{\boldsymbol{\nabla}}} n \cdot \underline{\hat{\boldsymbol{\nabla}}} m_z] \\
&= E_{xc}[\underline{\mathbf{P}}^{col}]
\end{aligned} \tag{60}$$

in which cl indicates the collinear limit of the argument.

Now for the remaining case of negative m_z, we start by looking at the behaviour of the collinear expression. From Eq. (57), we obtain the following:

$$\begin{aligned}
&E_{xc}[\underline{\mathbf{P}}^{col}] \\
&= E_{xc}[n, m_z, \underline{\hat{\boldsymbol{\nabla}}} n \cdot \underline{\hat{\boldsymbol{\nabla}}} n, \underline{\hat{\boldsymbol{\nabla}}} m_z \cdot \underline{\hat{\boldsymbol{\nabla}}} m_z, \underline{\hat{\boldsymbol{\nabla}}} n \cdot \underline{\hat{\boldsymbol{\nabla}}} m_z] \\
&\underbrace{=}_{m_z < 0} E_{xc}[n, -|m_z|, \underline{\hat{\boldsymbol{\nabla}}} n \cdot \underline{\hat{\boldsymbol{\nabla}}} n, \underline{\hat{\boldsymbol{\nabla}}} |m_z| \cdot \underline{\hat{\boldsymbol{\nabla}}} |m_z|, -\underline{\hat{\boldsymbol{\nabla}}} n \cdot \underline{\hat{\boldsymbol{\nabla}}} |m_z|]
\end{aligned} \tag{61}$$

Comparing the third line of Eq. (60) with Eq. (61), we see that the correct collinear limit for the canonical NC formulation can be obtained provided that:

$$\begin{aligned}
&E_{xc}[n, |m_z|, \underline{\hat{\boldsymbol{\nabla}}} n \cdot \underline{\hat{\boldsymbol{\nabla}}} n, \underline{\hat{\boldsymbol{\nabla}}} |m_z| \cdot \underline{\hat{\boldsymbol{\nabla}}} |m_z|, \underline{\hat{\boldsymbol{\nabla}}} n \cdot \underline{\hat{\boldsymbol{\nabla}}} |m_z|] = \\
&E_{xc}[n, -|m_z|, \underline{\hat{\boldsymbol{\nabla}}} n \cdot \underline{\hat{\boldsymbol{\nabla}}} n, \underline{\hat{\boldsymbol{\nabla}}} |m_z| \cdot \underline{\hat{\boldsymbol{\nabla}}} |m_z|, -\underline{\hat{\boldsymbol{\nabla}}} n \cdot \underline{\hat{\boldsymbol{\nabla}}} |m_z|]
\end{aligned} \tag{62}$$

The key passage is to now realize that Eq. (62) represents nothing other than the formal statement that the xc energy is invariant to a global rotation of the spin reference frame (i.e., a rotation of the spin-quantization axis) from the z direction to the $-z$ direction (or, equivalently, an interchange of all α labels for β labels, and vice-versa). Given that the expression for the xc energy functional originates from the theory of Von Barth and Hedin,[1] in which the choice of the orientation of the spin-quantisation axis is arbitrary, the xc energy expression is necessarily invariant to a global reorientation of the spin reference frame.

Combining Eqs. (60)-(62), we find that the xc energy expression from the canonical NC formulation has the correct collinear limit:

$$E_{xc}[\underline{\mathbf{P}}^{can}]\big|_{cl} = E_{xc}[\underline{\mathbf{P}}^{col}] \tag{63}$$

The rotational invariance of the xc energy from the canonical NC formulation can then be shown by choosing a different orientation for the spin-quantization axis,

invoking the invariance of the xc energy functional to a global rotation of the spin reference frame, and repeating the steps outlined in Eqs. (56)-(62) for the new orientation.

We now move on to showing the reduction to the collinear limit (and, as a consequence, also rotational invariance) of the xc energy expression for the case of the SF NC formulation. A similar demonstration to that provided above can be also shown for the SF formulation by first looking at the collinear limit of the individual gradient variables that are contained in the definition of $\underline{\mathbf{P}}^{sf}$ in Eq. (59):

$$\underline{\hat{\boldsymbol{\nabla}}} n \cdot \underline{\hat{\boldsymbol{\nabla}}} n \Big|_{cl} = \underline{\hat{\boldsymbol{\nabla}}} n \cdot \underline{\hat{\boldsymbol{\nabla}}} n \tag{64a}$$

$$\underline{\hat{\boldsymbol{\nabla}}}\ \underline{\mathbf{m}} \cdot \circ \underline{\hat{\boldsymbol{\nabla}}}\ \underline{\mathbf{m}} \Big|_{cl} = \underline{\hat{\boldsymbol{\nabla}}} m_z \cdot \underline{\hat{\boldsymbol{\nabla}}} m_z \tag{64b}$$

and:

$$\begin{aligned} f_{\nabla}\Xi|_{cl} &= \mathrm{sgn}\left[\underline{\hat{\boldsymbol{\nabla}}} n \cdot \left(\underline{\hat{\boldsymbol{\nabla}}} m_z\right) m_z\right] |\underline{\hat{\boldsymbol{\nabla}}} n \cdot \underline{\hat{\boldsymbol{\nabla}}} m_z| \\ &= \underline{\hat{\boldsymbol{\nabla}}} n \cdot \underline{\hat{\boldsymbol{\nabla}}} |m_z| \end{aligned} \tag{64c}$$

Substituting Eqs. (64a)-(64c) in Eq. (59) and proceeding as in Eqs. (60)-(61), we obtain the correct collinear limit also for the xc energy expression from the SF formulation:

$$E_{xc}[\underline{\mathbf{P}}^{sf}]\Big|_{cl} = E_{xc}[\underline{\mathbf{P}}^{col}] \tag{65}$$

We now consider the xc potential expressions. Their proper collinear limit and, consequently, rotational invariance, for both SF and canonical formulations now follows naturally by substituting Eqs. (63) and (65) in Eqs. (15)-(17):

$$\begin{aligned} \hat{\mathbf{V}}_{xc}\Big|_{cl} &= \frac{\delta E_{xc}[\underline{\mathbf{P}}^{i}]}{\delta n}\hat{\boldsymbol{\sigma}}_0 + \sum_c \frac{\delta E_{xc}[\underline{\mathbf{P}}^{i}]}{\delta m_c}\hat{\boldsymbol{\sigma}}_c\Big|_{cl} \\ &= \frac{\delta E_{xc}[\underline{\mathbf{P}}^{col}]}{\delta n}\hat{\boldsymbol{\sigma}}_0 + \frac{\delta E_{xc}[\underline{\mathbf{P}}^{col}]}{\delta m_z}\hat{\boldsymbol{\sigma}}_z \end{aligned} \tag{66}$$

4. On the Treatment of Unstable Terms of Non-Collinear Exchange-Correlation Potentials

We discuss here algorithmic strategies for the evaluation of delicate terms in the non-collinear xc potential. Several previous authors have acknowledged numerical issues associated with the evaluation of non-collinear xc potentials, particularly so for xc functionals beyond the LDA.[8–14,17,19,67] However, to the best of our knowledge, an effective screening algorithm for dealing with these problems in both the canonical and SF formulations is yet to be presented in the literature.

All of the difficulties previously noted in the literature are related to factors $R_c = m_c/m$, which are ill-defined at those points in space where the magnetization is small. Although, formally, the xc functionals and potential are everywhere finite, the problem lies in their accurate numerical evaluation. In general, the m_c/m factors appear both in the expressions for the variables on which GGA xc functionals depend and in the expression for the xc magnetic field (for all functionals, including LDA). In the canonical theory, the challenging terms occur in both the definition of the GGA variables – see Eq. (46) – and in the xc potential, see Eq. (50). For the theory of Scalmani and Frisch, the problematic terms do not occur in the definition of the GGA variables, but are still present in the definition of the xc magnetic field term of the potential in Eq. (55).

For LDA functionals, from Eqs. (17) and (44), points of small magnetization can be safely disregarded because the m_c/m factors in the potential multiply $\partial F_{xc}/\partial m$ which is also vanishing for vanishing m. This is not the case for GGA functionals, where the m_c/m factors sometimes multiply gradients of the magnetization, gradients of the total density, or gradients of the atomic orbitals, which are not necessarily small where m is small. See for example Eqs. (46) and (50) for the canonical theory.

As a consequence, the treatment of these terms requires a very careful local screening of the magnitude of the magnetization m and of its individual Cartesian components m_c at each point of the DFT grid. Here we introduce a screening algorithm that can be used with any non-collinear formulation and sketch its main features. The algorithm is presented for the case where the m_c/m terms multiply gradients of the magnetization but it can be very easily extended to the cases where the m_c/m factors multiply instead gradients of the total density or gradients of the atomic orbitals.

At each point in space (i.e. at each point of the DFT integration grid), the absolute value $|m_c|$ of the three Cartesian components of the magnetization $\underline{\mathbf{m}}$ are screened according to a threshold (here set to 10^{-27} a.u.). Two distinct cases are identified and treated differently: 1) all three components are individually smaller than the threshold, or 2) at least one component is larger than the threshold. We treat these two cases as follows:

1. The three components of the magnetization are all small. We locally set:

$$\begin{aligned} m &= 0\ ; \\ \underline{\hat{\boldsymbol{\nabla}}} m &= \sum_c \left\langle \frac{m_c}{m} \right\rangle \underline{\hat{\boldsymbol{\nabla}}} m_c\ , \end{aligned}$$

   where the gradient of the magnetization $\underline{\hat{\boldsymbol{\nabla}}} m$ at that point is expressed in terms of the gradients of the three Cartesian components of the magnetization at the same point $\underline{\hat{\boldsymbol{\nabla}}} m_c$ while the prefactors $\langle m_c/m \rangle$ are average values for m_c/m. In the present implementation, the mean quantities $\langle m_c/m \rangle$ are calculated by averaging the m_c/m over the atomic basin to which the current point of the DFT grid belongs. The size of each atomic basin is determined using the same atomic radii that

are used to calculate the DFT integration weights. These quantities are computed from the values of the magnetization of the previous iteration of the SCF (or of the starting guess at the first iteration). Other choices for the partitioning of space for calculating the averaged $\langle m_c/m \rangle$ quantities could be possible but we leave this to future work. These average values are essential to ensure numerical stability at those (many) points where the m_c and m are so small that their ratio could not be evaluated with any reasonable degree of confidence. Moreover, they are also useful when m_c is too small to reasonably determine its sign (positive or negative). For these reasons, it is beneficial to instead associate an average value to m_c/m calculated over the atomic basin of the current point in space.

2. At least one of the three Cartesian components of the magnetization is large in absolute value. The largest component, in absolute value, is determined and the following signed quantity defined:

$$m_{max} = \mathrm{sgn}\left(m_x + m_y + m_z\right) \times \max\left(\left|m_x\right|,\left|m_y\right|,\left|m_z\right|\right) \ .$$

At this point, a screening on the "local collinearity" is performed. The absolute value of the other two, non-maximum, components of the magnetization is checked relative to $|m_{max}|$. Two distinct cases are identified, which are treated differently:

(a) Both non-maximum Cartesian components are small relative to $|m_{max}|$ and therefore the system is locally collinear. The two small components are put to zero and the problem reduces to the collinear one with the quantization axis along $|m_{max}|$. In this case we set:

$$m = |m_{max}| \ ,$$
$$\underline{\hat{\mathbf{\nabla}}} m = \mathrm{sgn}(m_{max}) \underline{\hat{\mathbf{\nabla}}} m_{max} \ .$$

(b) At least one of the non-maximum Cartesian components is not small relative to $|m_{max}|$. In this case, we set explicitly:

$$m = \sqrt{m_x^2 + m_y^2 + m_z^2} \ ,$$
$$\underline{\hat{\mathbf{\nabla}}} m = \sum_c R_c \underline{\hat{\mathbf{\nabla}}} m_c \ ,$$

where the factors R_c are determined as follows, based on the value of the ratios $|m_c|/m$: if the ratio $|m_c|/m$ is small than we set $R_c = 0$, otherwise we set it to $R_c = m_c/m$.

III. COMPUTATIONAL DETAILS

We have implemented all of the DFT formulations discussed above in a developmental version of the CRYSTAL17 code.[57] To validate our implementation and discuss numerical strategies for its use, we have chosen a test set of small molecular systems, and have performed similar calculations also with the latest public version of the DIRAC[69] and TURBOMOLE[70] codes. Both SR and SOC effects are treated from RECPs. The systems are similar to those discussed in Part I.[58] That is, the I_2, CH_3I, IH and TlBr molecules, in both a neutral state (closed-shell electronic configurations) and a positively charged state obtained by removing one electron from the molecules (open-shell electronic configurations): namely, I_2^+, CH_3I^+, IH^+ and $TlBr^+$. We refer the reader to Part I for details on the used basis sets, RECPs and molecular geometries.

The numerical integration required for calculating the xc energy and matrix elements was achieved with our implementation on an unpruned grid. For the comparison with other implementations, this grid (denoted as G1) contained 75 radial points and a Lebedev accuracy level of 16, corresponding to 974 angular points for each radial point.[71–73] The quadrature weights proposed by Becke were used in all calculations.[74] For calculations with the DIRAC and TURBOMOLE codes, the finest available grids were used, which are similar to the one chosen with our implementation and all integral screenings were deactivated. The SCF procedures with all codes were converged down to a criterion on the energy of 1×10^{-9} Hartree a.u. (Ha). Calculations were performed with the SVWN5 LDA functional,[75,76] The PBE GGA functional,[77] and the PBE0 and B3LYP hybrid-GGA functionals.[78,79] The guess for the SCF procedure was generated from a superposition of SR atomic-HF density matrices using an approach described in Ref. 80. The magnetization generated from each of the atomic SR density matrices is rotated along a desired direction using an approach described in Part I.[58]

For the tests that were performed with only our implementation, we used a finer numerical DFT grid (denoted as G2) consisting of 500 radial points and a Lebedev accuracy level of 29, corresponding to 5810 angular points and a criterion on the energy for convergence of the SCF of 1×10^{-12} Ha (unless explicitly stated otherwise). More specific details are provided in the electronic supplementary information (ESI), in which example input decks are provided.[81]

IV. RESULTS AND DISCUSSION

We discuss below several aspects of the methodologies formally illustrated in Section II: i) we compare our implementation to those available in other codes; ii) we document the reduction to the collinear limit of different non-collinear formulations of the DFT; iii) we quantify the degree of rotational invariance of different non-collinear formulations.

TABLE I. Energies for the closed-shell electronic configurations. The $\Delta E_{SOC} = E_{SOC} - E_0$ is the SOC contribution to the energy as obtained with our implementation. The $\Delta\Delta E_X = \Delta E_X - \Delta E_{SOC}$ is the difference between the SOC energy contribution computed with the program X=TUR or DIR (where TUR stands for TURBOMOLE and DIR stands for DIRAC) and that with our implementation in CRYSTAL17. All quantities are reported in atomic units (Ha).

	I_2	CH_3I	IH	TlBr
LDA				
ΔE_{SOC}	-7.7×10^{-3}	-3.2×10^{-3}	-3.0×10^{-3}	-3.6×10^{-2}
$\Delta\Delta E_{DIR}$	$+4.8\times10^{-9}$	$+4.0\times10^{-9}$	$+1.0\times10^{-9}$	-
$\Delta\Delta E_{TUR}$	$+1.2\times10^{-5}$	$+1.3\times10^{-6}$	$+6.9\times10^{-7}$	$+2.6\times10^{-6}$
PBE				
ΔE_{SOC}	-7.9×10^{-3}	-3.2×10^{-3}	-3.0×10^{-3}	-3.5×10^{-2}
$\Delta\Delta E_{DIR}$	$+1.3\times10^{-8}$	$+1.8\times10^{-9}$	$+2.1\times10^{-9}$	-
$\Delta\Delta E_{TUR}$	$+1.4\times10^{-5}$	$+1.4\times10^{-6}$	$+2.9\times10^{-7}$	$+2.5\times10^{-6}$
PBE0				
ΔE_{SOC}	-7.7×10^{-3}	-3.1×10^{-3}	-2.9×10^{-3}	-3.4×10^{-2}
$\Delta\Delta E_{DIR}$	$+1.1\times10^{-8}$	$+1.1\times10^{-9}$	$+1.9\times10^{-9}$	-
$\Delta\Delta E_{TUR}$	$+1.3\times10^{-5}$	$+1.0\times10^{-6}$	$+3.6\times10^{-7}$	$+1.9\times10^{-6}$

TABLE II. Energies for the open-shell electronic configurations. See caption of Table I for a definition of all quantities. Values are given in atomic units (Ha). Calculations are performed with the canonical non-collinear theory described in section II D 1.

	I_2^+	CH_3I^+	IH^+	$TlBr^+$
LDA				
ΔE_{SOC}	-2.2×10^{-2}	-1.6×10^{-2}	-1.6×10^{-2}	-4.2×10^{-2}
$\Delta\Delta E_{TUR}$	$+8.9\times10^{-5}$	$+5.6\times10^{-4}$	$+1.3\times10^{-4}$	$+4.1\times10^{-3}$
PBE				
ΔE_{SOC}	-2.1×10^{-2}	-1.4×10^{-2}	-1.4×10^{-2}	-3.9×10^{-2}
$\Delta\Delta E_{TUR}$	$+9.6\times10^{-5}$	$+3.7\times10^{-4}$	$+1.4\times10^{-4}$	$+1.3\times10^{-3}$
PBE0				
ΔE_{SOC}	-2.1×10^{-2}	-1.4×10^{-2}	-1.4×10^{-2}	-3.9×10^{-2}
$\Delta\Delta E_{TUR}$	$+1.1\times10^{-4}$	$+3.4\times10^{-4}$	$+1.5\times10^{-4}$	$+2.1\times10^{-3}$

A. Comparison with Previous Implementations

We first report comparisons of our implementation with those available in the DIRAC and TURBOMOLE codes, for validation purposes. We start by discussing results on the closed-shell electronic configurations, where since the magnetization is vanishing, and, as a consequence, in Eq. (17) $\delta E_{xc}/\delta\underline{\mathbf{m}} = \underline{\mathbf{0}}$, and all of the formulations coincide. The closed-shell tests thus permit to test aspects of the implementations that are not related to the treatment of non-collinear magnetization (e.g. the integration grid, accuracy of the evaluation of electron repulsion integrals and the implementation of the xc functionals and their derivatives). Calculations were performed with and without the SOC operator included in the Hamiltonian, and the energy differences of these two calculations, ΔE_{SOC}, are tabulated.

In Table I, we report the ΔE_{SOC} calculated with our implementation, as well as the differences of the ΔE_{SOC} with respect to those calculated with the other implementations. These are denoted in the table as $\Delta\Delta E_X$, where X denotes the code used for the calculation, that is X = TUR or DIR. It can be seen from the table that the agreement with DIRAC is very satisfactory in all cases, because the $\Delta\Delta E_{DIR}$ is always on the order of 1×10^{-9} Ha, which is remarkably the same accuracy as the convergence of the SCF. The only exception is the PBE or PBE0 calculations on I_2, where the $\Delta\Delta E_{DIR}$ is instead on the order of 1×10^{-8} Ha.

As was also noted in Part I,[58] for the case of TlBr, it was not possible to use the DIRAC code in exactly the same computational conditions as in the other codes. This is due to the fact that the RECP-SOC implementation in DIRAC is only available with a basis of Cartesian Gaussian-type functions that differ from spherical Gaussian-type functions (used in our implementation as well as in the TURBOMOLE one) starting from angular momentum $l = 2$ (i.e. starting from d-type functions). Given that TlBr has occupied d orbitals in the valence, it was not possible to perform the comparison with DIRAC in this case. For all other molecular systems, no $l = 2$ or higher angular momentum functions were included in the valence basis sets, so that we were able to perform the comparison.

The agreement with TURBOMOLE is still very satisfactory but less good because this implementation uses the resolution of identity (RI) approximation for at least the evaluation of the Coulomb integrals. The RI approximation introduces inaccuracies which do not perfectly cancel between the calculations with and without SOC. As such, the $\Delta\Delta E_{TUR}$ are on the order of 1×10^{-5} Ha (for the I_2 molecule) to 1×10^{-7} Ha (for the IH molecule). These values are however still more than sufficient to confirm the correctness of the implementation, being two to four orders of magnitude smaller than the SOC contribution to the energy. The agreement with both codes is generally better with LDA (where only the density needs to be evaluated on the numerical grid), or with PBE0 (which includes a significant portion of Fock exchange, and hence is in a larger part analytical). A worst agreement is generally found using PBE, where both the density and its gradient need to be evaluated on the numerical grid.

We now discuss the calculations on the open-shell elec-

tronic configurations, which are obtained by removing one electron from the same molecules discussed above. As in Part I, we were unable to perform comparable calculations with the DIRAC code on open-shell electronic configurations as, to the best of our knowledge, it is not possible to perform single-determinant Kramers-unrestricted calculations with the DIRAC code at present. So the comparison can only be made against the TURBOMOLE code. What is more, we are only able to use one formulation for each functional, using the TURBOMOLE code. That is, the canonical non-collinear formulation. The comparison of calculations done with both implementations is reported in Table II. It can be seen from Tables I and II that the SOC contribution to the total energy, ΔE_{SOC}, is now increased by a factor of three to four by removing one electron from all systems, except for TlBr, where the ΔE_{SOC} instead only increases by about 10%. A similar result was reported in Part I with the HF theory. The comparison with the TURBOMOLE implementation is now slightly less impressive than for the closed-shell systems, because the evaluation of the xc matrix elements and potential now also requires a numerical integration containing functions of the magnetization (and possibly its gradient) and not only the density. The $\Delta\Delta E_{TUR}$ is now mostly on the order of 1×10^{-4} Ha, except for $TlBr^+$, where it is instead on the order of 1×10^{-3} Ha. We note, however that the $\Delta\Delta E_{TUR}$ is still at least one order of magnitude smaller (in absolute value) than the ΔE_{SOC}, which helps confirm the correctness of the implementations.

The reported effect of SOC on the total energies of the positively charged ions in Table II is also reflected in associated changes to their valence properties. Tables S1 and S2 quantify the changes in the particle-number n and z-component magnetization m_z Mulliken populations, reported as differences from the calculations with/without SOC for the positively charged open-shell systems. Fig. S1 provides the associated changes in the orbital energy levels, for states lying close to the HOMO. These tables and figure show that the changes in the total energies from SOC have considerable effect on the valence properties of the molecules, as reflected, for example, in significant changes to the HOMO-LUMO gaps. Table S1 shows the effect of the xc functional on the changes in the n and m_z Mulliken populations of $TlBr^+$ induced by SOC. It is seen that the PBE0 calculations induce changes in the populations on the order of 10^{-1} a.u. from SOC, while the LDA and PBE ones only induce changes on the order of 10^{-3} a.u. Indeed, given that the PBE0 functional includes a non-vanishing fraction of Fock exchange, it allows to include the SOC-induced orbital- and spin-current densities in the definition of the electron-electron potential,[28,59] which may lead to larger SOC-induced changes in the valence properties of the molecules.

TABLE III. Deviation from the collinear limit of various non-collinear formulations (CAN stands for "canonical" and SF for "Scalmani-Frisch" described in sections II D 1 and II D 2, respectively). The quantization axis is along the xyz diagonal. The reported quantities are energy differences (in atomic units) between non-collinear formulations and the collinear one for the open-shell electronic configurations in the absence of SOC.

	I_2^+	CH_3I^+	IH^+	$TlBr^+$
LDA				
CAN/SF	-4.7×10^{-13}	$+2.3\times10^{-13}$	-2.0×10^{-14}	$+1.1\times10^{-12}$
PBE				
CAN	$+6.9\times10^{-13}$	-7.1×10^{-14}	$+4.1\times10^{-12}$	-2.8×10^{-13}
SF	$+2.5\times10^{-14}$	-5.8×10^{-13}	$+3.0\times10^{-15}$	$+5.7\times10^{-14}$
PBE0				
CAN	$+1.3\times10^{-12}$	$+8.5\times10^{-12}$	$+1.5\times10^{-12}$	$+1.7\times10^{-11}$
SF	-1.1×10^{-14}	-2.5×10^{-13}	$+7.0\times10^{-15}$	-1.1×10^{-13}
B3LYP				
CAN	$+2.5\times10^{-12}$	-1.4×10^{-11}	$+6.0\times10^{-14}$	-2.6×10^{-13}
SF	-1.0×10^{-12}	-1.3×10^{-11}	-5.0×10^{-15}	-3.1×10^{-13}

B. The Reduction to the Collinear Limit of Non-Collinear Theories

We discuss now the reduction to the collinear limit of non-collinear formulations of the DFT, that is the ability of non-collinear theories to provide the same energy of the collinear theory in those cases where the magnetization is everywhere collinear. To do so, we consider the four open-shell systems without SOC (i.e. in the absence of any torque that can rotate the initial magnetization) so that the magnetization remains aligned to the direction along which it was pointing in the collinear guess.

Table III reports the energy differences between the collinear theory and the different NC formulations (CAN stands for "canonical", SF for "Scalmani-Frisch"). The table supports the formal analysis provided in section II D 3. Indeed, it is seen that both NC formulations yield energy differences with respect to the collinear one that are very small, being on the order of 10^{-15} to 10^{-11} Ha (for comparison the tolerance on the energy for convergence of the SCF procedure was 10^{-12} Ha, as stated in section III). The reported energy differences are smaller for the Scalmani-Frisch formulation rather than the canonical one. This is expected from the considerations outlined in section II D 4, in which it was pointed out that the delicate m_c/m terms that can lead to numerical instabilities occur in the expressions for both the xc energy and potential in the CAN formulation, but only in the potential for the SF formulation. This results in

the SF formulation being slightly more numerically stable than the CAN one, which is demonstrated in the smaller energy differences reported in table III. However, given that the energy differences never exceed a value on the order of 10^{-11} Ha, we can conclude from table III that both NC formulations are more than adequate from the point of view of reduction to the collinear limit for total energy calculations.

C. The Rotational Invariance of Non-Collinear Theories

We now discuss the rotational invariance of the collinear approach and of the various non-collinear formulations, in the presence of SOC. The tests are performed on the I_2^+ linear molecule, for which seven different orientations are explored: from parallel to the z axis, 0°, to parallel to the x axis, 90°. At each orientation, an initial atomic guess for the magnetization is used, which is parallel to the molecular axis. The absolute differences between the energies of the various orientations with respect to that obtained when the molecule is along z (taken as a reference) are reported in Table IV for the plain GGA functional PBE and hybrid GGA functionals PBE0 and B3LYP, or Table V for the LDA functional. The last row of both tables reports average energy differences over all the explored orientations. For perfectly rotationally invariant formulations of the theory the reported energy differences should be vanishingly small. To quantify the effect of the numerical grid on the rotational invariance, Table S3 of the ESI provides further calculations with the different formulations for GGA functionals, in which the smaller G1 numerical grid was used instead of the finer G2 grid. Furthermore, Table S4 of the ESI provides GGA calculations in which the SOC operator was excluded from the Hamiltonian.

TABLE IV. Rotational invariance of GGA collinear and non-collinear formulations of DFT with SOC. The linear I_2^+ molecule is studied in seven different orientations (from parallel to the z axis, 0°, to the x axis, 90°). The atomic guess magnetization is always parallel to the axis of the molecule. For each orientation, the absolute difference (in Ha) between the computed energy and that obtained when the molecule is along z ($|E - E_z|$), and the number of cycles needed to converge the SCF are reported. The last row reports the average over all the explored orientations, |av|, of the absolute value of the quantities in their respective columns.

	Collinear				Non-Collinear									
					Canonical						Scalmani-Frisch			
	PBE		PBE0		PBE		PBE0		B3LYP		PBE		PBE0		B3LYP	
0°	Ref.	52	Ref.	68	Ref.	65	Ref.	97	Ref.	91	Ref.	53	Ref.	78	Ref.	73
10°	7.7×10^{-05}	52	6.3×10^{-05}	113	4.2×10^{-09}	70	2.1×10^{-09}	110	5.8×10^{-09}	101	2.3×10^{-09}	58	5.5×10^{-09}	107	1.8×10^{-09}	100
22°	3.9×10^{-04}	52	3.1×10^{-04}	131	1.3×10^{-09}	65	3.3×10^{-09}	124	5.1×10^{-09}	118	2.3×10^{-09}	65	7.7×10^{-10}	125	1.1×10^{-09}	115
45°	1.5×10^{-03}	53	1.2×10^{-03}	182	2.7×10^{-10}	69	8.2×10^{-09}	134	4.1×10^{-08}	114	4.7×10^{-10}	68	5.7×10^{-09}	133	2.0×10^{-09}	124
68°	3.1×10^{-03}	72	1.1×10^{-03}	1437	7.2×10^{-10}	65	2.8×10^{-09}	115	5.6×10^{-09}	116	1.7×10^{-09}	65	1.4×10^{-09}	124	5.9×10^{-10}	115
80°	1.7×10^{-03}	194	9.6×10^{-04}	950	4.1×10^{-09}	70	2.0×10^{-09}	110	5.9×10^{-09}	101	2.4×10^{-09}	56	1.5×10^{-10}	107	2.0×10^{-09}	98
90°	1.6×10^{-03}	51	3.2×10^{-03}	82	1.5×10^{-10}	65	1.5×10^{-10}	97	1.5×10^{-10}	91	1.6×10^{-10}	54	5.6×10^{-09}	78	1.6×10^{-10}	73
|av|	1.4×10^{-03}	78	1.1×10^{-03}	423	1.8×10^{-09}	67	3.1×10^{-09}	112	9.1×10^{-09}	105	1.5×10^{-09}	60	3.2×10^{-09}	107	1.1×10^{-09}	100

From the tables IV and V, it is clear that, as expected, the collinear approach does not ensure rotational invariance when the SOC operator is included in the Hamiltonian, both at the LDA and GGA level. Indeed, the average deviation of the energy among different orientations is very large, on the order of 1×10^{-3} Ha for LDA, PBE and PBE0. This lack of rotational invariance is also reflected in the amount of cycles required to converge the SCF for the different orientations, which shows very large variations for the different orientation. For the case of LDA, the rotational invariance is fully regained by the non-collinear formulation, as the average deviation becomes 2.2×10^{-10} Ha. It is interesting that almost identical values are obtained from both the SF and CAN formulations for GGA functionals without SOC (see Table S4), which confirms the numerical robustness of the NC GGA implementation.

Table IV shows that both formulations (CAN and SF)

TABLE V. Same as Table IV, but now results are reported for the LDA, using both the collinear or non-collinear theories, with and without the inclusion of the SOC operator in the Hamiltonian.

	Collinear				Non-Collinear			
	with SOC		without SOC		with SOC		without SOC	
0°	Ref.	49	Ref.	50	Ref.	50	Ref.	
10°	7.1×10^{-05}	49	5.0×10^{-11}	50	4.9×10^{-11}	56	5.0×10^{-11}	50
22°	3.6×10^{-04}	48	1.8×10^{-11}	50	1.6×10^{-11}	65	1.8×10^{-11}	50
45°	1.4×10^{-03}	48	4.4×10^{-10}	50	4.4×10^{-10}	65	4.4×10^{-10}	50
68°	2.1×10^{-03}	510	5.7×10^{-10}	50	5.7×10^{-10}	62	5.7×10^{-10}	50
80°	1.9×10^{-03}	273	5.7×10^{-11}	50	5.9×10^{-11}	56	5.7×10^{-11}	50
90°	1.9×10^{-03}	48	1.6×10^{-10}	51	1.6×10^{-10}	51	1.6×10^{-10}	50
|av|	1.3×10^{-03}	146	2.2×10^{-10}	50	2.2×10^{-10}	58	2.2×10^{-10}	50

for NC GGA calculations also allow to restore the rotational invariance of the calculation when a SOC operator is included in the Hamiltonian, with the average deviation of the energy being however about an order of magnitude higher than for LDA calculations, at 1.5-3.2 $\times10^{-9}$ for PBE and PBE0, and 1.1-9.1 $\times10^{-9}$ for B3LYP. A greater amount of SCF cycles is required to converge the PBE0 calculations as compared to the PBE ones, which results in slightly larger average deviations of the total energy (1.8 $\times10^{-9}$ Ha for PBE vs. 3.1 $\times10^{-9}$ Ha for PBE0 and the CAN formulation). Both the CAN and SF formulations of PBE and PBE0 achieve essentially identical degrees of rotational invariance with the finer G2 numerical grid used for the calculations in table IV, as the reported average deviations of the total energy are very similar for both formulations. The results in Table S3, however show that the SF formulation is confirmed to be slightly more numerically stable than the CAN one when the coarser G1 numerical grid is used, because energy deviations are slightly smaller (e.g., 7.7×10^{-8} Ha with the SF formulation vs. 1.3×10^{-7} Ha with the CAN formulation for the PBE functional). From Table IV, the SF formulation also appears more stable for the B3LYP calculations with the G2 grid, as the energy deviation is lower by almost an order of magnitude (e.g., 1.1×10^{-9} Ha with the SF formulation vs. 9.1×10^{-9} Ha with the CAN formulation). The superior numerical stability of the SF formulation is also reflected in the lower number of cycles required to converge the SCF, as compared to the CAN formulation. In the most extreme case (G1 grid, PBE functional) the SCF is converged at an average of 9 cycles faster with the SF formulation, as convergence of the SCF took an average of 61 cycles for the SF formulation instead of 70 cycles for the CAN one (see last row of Table S3). However, given that the average deviations of the energies in Table IV are similar for both the SF and CAN formulations, we can conclude that also from the point of view of rotational invariance both formulations are more than adequate for total energy calculations.

Further insight into how the NC GGA implementation allows to restore the rotational invariance can be obtained by looking at Figure 1. This Figure provides contour plots of the magnetization from the PBE calculations as the molecule is rotated from the x axis (right of the Figure) to the z axis (left of the Figure). The top row of the Figure shows that the magnetizations obtained from the collinear formulation, and the two other rows provide those from the CAN NC and SF NC formulations. It is seen from those obtained by the collinear formulation that although the magnetizations were oriented along the molecular axis in the guess, they are partially rotated towards the z axis during the SCF procedure, such that the plotted arrows no longer point directly along the molecular axis. Instead, using the CAN or SF NC formulations, the magnetizations are seen to always remain along the molecular axis throughout the calculation, such that the plotted arrows rotate along with the molecule.

V. CONCLUSIONS

The formalism of Kramers-unrestricted collinear and all previously reported formulations of non-collinear density functional theory (DFT) for the self-consistent treatment of spin-orbit coupling (SOC) in electronic structure calculations has been revised. The various approaches have been implemented in the CRYSTAL program and have been compared both formally and using test examples on small molecules.

The formal analysis shows that all formulations for calculations in the non-collinear generalized-gradient approximation (GGA) formally reduce to the proper collinear limit and are, as a consequence, rotationally invariant. The illustrative calculations provide a first numerical comparison of both previously suggested non-collinear formulations for GGA functionals. They highlight the importance of using an effective screening algorithm for treating delicate terms that appear in the expressions for the exchange-correlation energy and/or potential. If the screening is achieved on a sufficiently fine grid, then all non-collinear GGA formulations are adequate for total energy calculations. The formulation

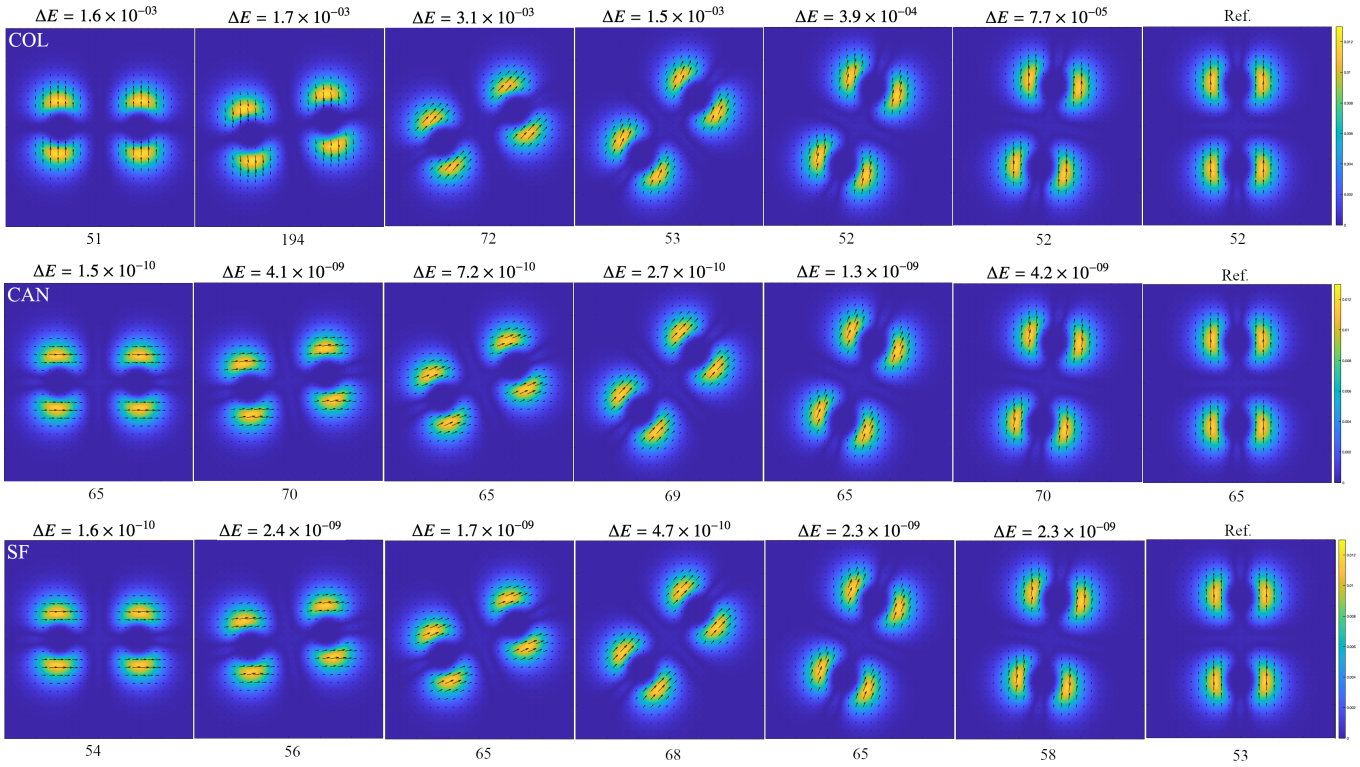

FIG. 1. Spatial distribution of the electronic magnetization for the I_2^+ molecule in the xz plane, as computed with the PBE xc functional, upon inclusion of SOC, with three formulations of the GGA theory: collinear COL, canonical CAN, and Scalmani-Frisch SF. The molecular axis and atomic guess magnetization is progressively rotated from the x axis (left) to the z axis (right). The small black arrows in the figure have lengths which reflect the magnitude and direction of the x and z components of the magnetization, while the color represents the magnitude m of the magnetization vector. The absolute value of the energy difference of each solution with respect to that obtained with the molecule along z is reported on top of the panels, as well as the number of cycles needed to converge the SCF, on the bottom of the panels. All quantities are reported in atomic units.

of Scalmani and Frisch is shown to be slightly more numerically stable (in terms of the consistency of energies obtained for different orientations of the molecules and reduction to the collinear limit) than the canonical formulation. However, the differences are very small and non-collinear GGA calculations including spin-orbit coupling can be performed with either formulation with a rotational invariance down to an order of 1.0×10^{-9} Ha, with the present implementation.

SUPPLEMENTARY MATERIAL

See Supplemental Material at URL for example input decks, a discussion of the effect of SOC on the eigenvalue spectrum and charge/spin populations of the open-shell molecules, and tables to quantify the rotational invariance of the formulations of non-collinear DFT for GGA functionals.

DATA AVAILABILITY STATEMENT

The data that supports the findings of this study are available within the article and its supplementary material.

ACKNOWLEDGEMENTS

J.K.D. is grateful to the National Science and Engineering Research Council of the Government of Canada for a Vanier scholarship and a Postdoctoral fellowship. Financial support was also received from the Slovak Research and Development Agency (Grant No. APVV-19-0516).

[1] U. von Barth and L. Hedin, J. Phys. C **5**, 1629 (1972).
[2] D. Grohol, K. Matan, J.-H. Cho, S.-H. Lee, J. W. Lynn, D. G. Nocera, and Y. S. Lee, Nat. mater. **4**, 323 (2005).
[3] K. Matan, D. Grohol, D. G. Nocera, T. Yildirim, A. B. Harris, S. H. Lee, S. E. Nagler, and Y. S. Lee, Phys. Rev. Lett. **96**, 247201 (2006).
[4] K. Matan, B. M. Bartlett, J. S. Helton, V. Sikolenko, S. Mat'aš, K. Prokeš, Y. Chen, J. W. Lynn, D. Grohol, T. Sato, et al., Phys. Rev. B **83**, 214406 (2011).

[5] P. Kurz, G. Bihlmayer, K. Hirai, and S. Blügel, Phys. Rev. Lett. **86**, 1106 (2001).
[6] Q. Cui, Q. Huang, J. A. Alonso, D. Sheptyakov, C. De la Cruz, M. Fernández-Díaz, N. Wang, Y. Cai, D. Li, X. Dong, et al., Phys. Rev. B **101**, 144424 (2020).
[7] J. Kubler, K.-H. Hock, J. Sticht, and A. Williams, J. Phys. F **18**, 469 (1988).
[8] I. W. Bulik, G. Scalmani, M. J. Frisch, and G. E. Scuseria, Phys. Rev. B **87**, 035117 (2013).
[9] J. E. Peralta, G. E. Scuseria, and M. J. Frisch, Phys. Rev. B **75**, 125119 (2007).
[10] D. Hobbs, G. Kresse, and J. Hafner, Phys. Rev. B **62**, 11556 (2000).
[11] G. Scalmani and M. J. Frisch, J. Chem. Theor. Comput. **8**, 2193 (2012).
[12] K. Knöpfle, L. Sandratskii, and J. Kübler, Phys. Rev. B **62**, 5564 (2000).
[13] V. García-Suárez, C. Newman, C. J. Lambert, J. Pruneda, and J. Ferrer, Eur. Phys. J. B **40**, 371 (2004).
[14] P. Kurz, F. Förster, L. Nordström, G. Bihlmayer, and S. Blügel, Phys. Rev. B **69**, 024415 (2004).
[15] A. Dal Corso and A. M. Conte, Phys. Rev. B **71**, 115106 (2005).
[16] M. K. Armbruster, F. Weigend, C. van Wüllen, and W. Klopper, Phys. Chem. Chem. Phys. **10**, 1748 (2008).
[17] F. Egidi, S. Sun, J. J. Goings, G. Scalmani, M. J. Frisch, and X. Li, J. Chem. Theor. Comput. **13**, 2591 (2017).
[18] C. Van Wüllen, J. Comput. Chem. **23**, 779 (2002).
[19] S. Komorovsky, P. J. Cherry, and M. Repisky, J. Chem. Phys. **151**, 184111 (2019).
[20] M. Repisky, S. Komorovsky, M. Kadek, L. Konecny, U. Ekström, E. Malkin, M. Kaupp, K. Ruud, O. L. Malkina, and V. G. Malkin, J. Chem. Phys. **152**, 184101 (2020).
[21] E. Engel, in *Theor. Comput. Chem.* (Elsevier, 2002), vol. 11, pp. 523–621.
[22] C. van Wüllen, in *Theor. Comput. Chem.* (Elsevier, 2004), vol. 14, pp. 598–655.
[23] J. Paquier and J. Toulouse, J. Chem. Phys. **149**, 174110 (2018).
[24] G. Vignale and M. Rasolt, Phys. Rev. B **37**, 10685 (1988).
[25] K. Bencheikh, J. Phys. A **36**, 11929 (2003).
[26] G. Vignale and M. Rasolt, Phys. Rev. Lett. **59**, 2360 (1987).
[27] E. Trushin and A. Görling, Phys. Rev. B **98**, 205137 (2018).
[28] J. K. Desmarais, J.-P. Flament, and A. Erba, Phys. Rev. B **102**, 235118 (2020).
[29] H. Englisch and R. Englisch, Phys. Status Solidi (b) **123**, 711 (1984).
[30] H. Englisch and R. Englisch, Phys. Status Solidi (b) **124**, 373 (1984).
[31] E. K. Gross, L. N. Oliveira, and W. Kohn, Phys. Rev. A **37**, 2809 (1988).
[32] E. K. Gross, L. N. Oliveira, and W. Kohn, Phys. Rev. A **37**, 2805 (1988).
[33] L. Oliveira, E. Gross, and W. Kohn, Phys. Rev. A **37**, 2821 (1988).
[34] P. Schipper, O. Gritsenko, and E. Baerends, Theor. Chem. Acc. **99**, 329 (1998).
[35] P. Schipper, O. Gritsenko, and E. Baerends, J. Chem. Phys. **111**, 4056 (1999).
[36] R. C. Morrison, J. Chem. Phys. **117**, 10506 (2002).
[37] L. N. Oliveira, E. K. Gross, and W. Kohn, Int. J. Quantum Chem. **38**, 707 (1990).
[38] C. Ullrich and W. Kohn, Phys. Rev. Lett. **87**, 093001 (2001).
[39] E. Pastorczak and K. Pernal, J. Chem. Phys. **140**, 18A514 (2014).
[40] O. Franck and E. Fromager, Mol. Phys. **112**, 1684 (2014).
[41] Z.-h. Yang, J. R. Trail, A. Pribram-Jones, K. Burke, R. J. Needs, and C. A. Ullrich, Phys. Rev. A **90**, 042501 (2014).
[42] A. Pribram-Jones, Z.-h. Yang, J. R. Trail, K. Burke, R. J. Needs, and C. A. Ullrich, J. Chem. Phys. **140**, 18A541 (2014).
[43] Z.-h. Yang, A. Pribram-Jones, K. Burke, and C. A. Ullrich, Phys. Rev. Lett. **119**, 033003 (2017).
[44] F. Sagredo and K. Burke, J. Chem. Phys. **149**, 134103 (2018).
[45] M. Filatov, Wiley Interdiscip. Rev. Comput. Mol. Sci. **5**, 146 (2015).
[46] M. Filatov, M. Huix-Rotllant, and I. Burghardt, J. Chem. Phys. **142**, 184104 (2015).
[47] W. Liu and Y. Xiao, Chem. Soc. Rev. **47**, 4481 (2018).
[48] F. Wang and T. Ziegler, J. Chem. Phys. **121**, 12191 (2004).
[49] F. Wang and T. Ziegler, J. Chem. Phys. **122**, 074109 (2005).
[50] M. Huix-Rotllant, B. Natarajan, A. Ipatov, C. M. Wawire, T. Deutsch, and M. E. Casida, PCCP **12**, 12811 (2010).
[51] Z. Rinkevicius and H. Ågren, Chem. Phys. Lett. **491**, 132 (2010).
[52] Z. Rinkevicius, O. Vahtras, and H. Ågren, J. Chem. Phys. **133**, 114104 (2010).
[53] Z. Li and W. Liu, J. Chem. Phys. **136**, 024107 (2012).
[54] J. Anton, B. Fricke, and E. Engel, Phys. Rev. A **69**, 012505 (2004).
[55] S. Komorovsky, M. Repisky, E. Malkin, T. B. Demissie, and K. Ruud, J. Chem. Theor. Comput. **11**, 3729 (2015).
[56] T. F. Stetina, J. M. Kasper, and X. Li, J. Chem. Phys. **150**, 234103 (2019).
[57] R. Dovesi, A. Erba, R. Orlando, C. M. Zicovich-Wilson, B. Civalleri, L. Maschio, M. Rérat, S. Casassa, J. Baima, S. Salustro, et al., WIREs Comput. Mol. Sci. **8**, e1360 (2018).
[58] J. K. Desmarais, J.-P. Flament, and A. Erba, J. Chem. Phys. **151**, 074107 (2019).
[59] J. Desmarais, J. Flament, and A. Erba, J. Phys. Chem. Lett. **10**, 3580 (2019).
[60] J. K. Desmarais, J.-P. Flament, and A. Erba, Phys. Rev. B **101**, 235142 (2020).
[61] H. Stoll, B. Metz, and M. Dolg, J. Comput. Chem. **23**, 767 (2002).
[62] L. Maron and C. Teichteil, Chem. Phys. **237**, 105 (1998).
[63] J. K. Desmarais, A. Erba, and R. Dovesi, Theor. Chem. Acc. **137**, 28 (2018).
[64] Z. Zhang, Theor. Chem. Acc. **133**, 1588 (2014).
[65] K. Capelle, G. Vignale, and B. Györffy, Phys. Rev. Lett. **87**, 206403 (2001).
[66] S. Sharma, J. Dewhurst, C. Ambrosch-Draxl, S. Kurth, N. Helbig, S. Pittalis, S. Shallcross, L. Nordström, and E. Gross, Phys. Rev. Lett. **98**, 196405 (2007).
[67] A. Petrone, D. B. Williams-Young, S. Sun, T. F. Stetina, and X. Li, Eur. Phys. J. B **91**, 169 (2018).
[68] J. A. Pople, P. M. Gill, and B. G. Johnson, Chem. Phys. Lett. **199**, 557 (1992).
[69] DIRAC, a relativistic ab initio electronic structure program, Release DIRAC17 (2017), written by L. Visscher, H. J. Aa. Jensen, R. Bast, T. Saue, and others (see `http://www.diracprogram.org`).
[70] *TURBOMOLE V7.3 2018, a development of University of Karlsruhe and Forschungszentrum Karlsruhe GmbH, 1989-2007, TURBOMOLE GmbH, since 2007; available from* `http://www.turbomole.com`.
[71] M. D. Towler, A. Zupan, and M. Causà, Comput. Phys. Comm. **98**, 181 (1996).
[72] V. I. Lebedev, USSR Comput. Math. Math. Phys. **16**, 10 (1976).
[73] V. I. Lebedev, Siber. Math. J. **18**, 99 (1977).
[74] A. D. Becke, J. Chem. Phys. **88**, 1053 (1988).
[75] P. A. Dirac, in *Math. Proc. Camb. Philo. Soc.* (Cambridge University Press, 1930), vol. 26, pp. 376–385.
[76] S. H. Vosko, L. Wilk, and M. Nusair, Can. J. Phys. **58**, 1200 (1980).
[77] J. P. Perdew, K. Burke, and M. Ernzerhof, Phys. Rev. Lett. **77**, 3865 (1996).
[78] C. Adamo and V. Barone, J. Chem. Phys. **110**, 6158 (1999).
[79] A. D. Becke, J. Chem. Phys. **98**, 5648 (1993).
[80] E. Clementi, *Modern techniques in computational chemistry: MOTECC-91*, vol. 91 (Springer Science & Business Media, 1991).
[81] See Supplemental Material at URL for example input decks, a discussion of the effect of SOC on the eigenvalue spectrum and charge/spin populations of the open-shell molecules and tables

to quantify the rotational invariance of the formulations of non-collinear DFT for GGA functionals.